72 pgs

ACR No. L4E13

L-665

NATIONAL ADVISORY COMMITTEE FOR AERONAUTICS

WARTIME REPORT

ORIGINALLY ISSUED
May 1944 as
Advance Confidential Report L4E13

ANALYSIS OF AVAILABLE DATA ON CONTROL SURFACES

HAVING PLAIN-OVERHANG AND FRISE BALANCES

By Paul E. Purser and Thomas A. Toll

Langley Memorial Aeronautical Laboratory
Langley Field, Va.

NACA

WASHINGTON

NATIONAL ADVISORY COMMITTEE FOR AERONAUTICS

ADVANCE CONFIDENTIAL REPORT

ANALYSIS OF AVAILABLE DATA ON CONTROL SURFACES

HAVING PLAIN-OVERHANG AND FRISE BALANCES

By Paul E. Purser and Thomas A. Toll

SUMMARY

The available data on control surfaces having plain-overhang and Frise balances have been analyzed and some empirical relations that will facilitate the prediction of the characteristics of balanced control surfaces from the geometric constants have been determined. The analysis presented has been limited to the effects of overhang, nose shape, gap, and Mach number. Although the relations given are not considered sufficiently reliable to allow satisfactory prediction of airplane stick forces without the aid of wind-tunnel tests of a scale model, they are considered applicable to the preliminary design of control-surface balances and to modifications of balances already in use.

The effects of balance variations in changing the slope of the curve of hinge-moment coefficient plotted against control-surface deflection and in changing the lift effectiveness of the control surface are correlated for low Mach numbers by a balance factor that accounts for the length and shape of overhang. No such factor was obtained that would adequately account for all of the variables affecting the slope of the curve of hinge-moment coefficient plotted against angle of attack or the deflection range over which the balance is effective in reducing the slope of the hinge-moment curve. The effects of gap and Mach number are presented for a few representative models. Some representative pressure-distribution diagrams are presented for controls with plain-overhang and Frise balances.

INTRODUCTION

The demands for more maneuverability and smaller control forces for high-speed combat aircraft and the

general increase in the size and speed of all types of
airplane have resulted in a considerable amount of re-
search on means for balancing control surfaces. The
results of a great part of the control-surface research
have recently been collected in two papers: one gener-
ally applicable to ailerons (reference 1), and the other
generally applicable to tail surfaces (reference 2).
The data contained in the two collections and in other
papers are being analyzed, correlated, and summarized at
LMAL. The results of these studies are being published
separately as they are completed. Reference 3 contains
information on internally balanced controls, reference 4
contains information on controls with beveled trailing
edges and similar contour modifications, and reference 5
contains data on horn-balanced controls.

The present paper deals with control surfaces
having plain-overhang and Frise balances. The effects
of overhang, nose shape, gap, and Mach number have been
studied. The Frise balance is considered only as a
special type of overhang balance, and certain charac-
teristics generally associated only with Frise balances -
such as the effects of bulges, vent gaps, slot shapes,
and the vertical locations of the hinge axes - have not
been considered. Such effects may sometimes be appre-
ciable, but they cannot be properly evaluated from the
existing data.

SYMBOLS

The coefficients, parameters, factors, and symbols
used in correlating and presenting the data are:

C_L lift coefficient

c_l section lift coefficient

C_{L_1} average lift coefficient over control-surface
               span for airfoil with plain sealed control
               surface

c_{l_1} section lift coefficient for airfoil with plain
               sealed control surface

C_h hinge-moment coefficient

c_h section hinge-moment coefficient

P pressure coefficient $\left(\dfrac{p - p_0}{q}\right)$

p local static pressure

p_0 static pressure in undisturbed airstream

q dynamic pressure of undisturbed airstream $\left(\dfrac{1}{2}\rho V^2\right)$

α angle of attack, degrees

δ_f control-surface deflection relative to airfoil, degrees

δ_{cr} critical control-surface deflection; that is, deflection at which plain-overhang or Frise balance is no longer effective in reducing slope of hinge-moment curve (approximately the deflection at which maximum lift is obtained for a given angle of attack)

c airfoil chord

$\bar{c}$ root-mean-square airfoil chord over span of control surface

c_f control-surface chord back of hinge line

$\bar{c}_f$ root-mean-square control-surface chord

c_b balance chord, distance from hinge line to leading edge of plain-overhang or Frise balance

$\bar{c}_b$ root-mean-square balance chord

c_b' contour balance chord, distance from hinge line to point of tangency of balance leading-edge arc and airfoil contour

$\bar{c}_b'$ root-mean-square contour balance chord

t thickness of airfoil section at hinge line

$\bar{t}$ root-mean-square of airfoil section thickness at hinge line

b_f span of control surface

b_b span of plain-overhang or Frise balance

A   aspect ratio

λ ratio of tip chord to root chord

M   Mach number; with subscripts, area moment of the balance profile about hinge axis

R   Reynolds number; with subscripts, balance nose radius

l chord-wise location of minimum-pressure point for low-drag airfoils measured in airfoil chords from leading edge (one-tenth of second digit in low-drag airfoil designation, reference 6)

F_1 overhang factor

F_2, F_2' nose-shape factors

K_1 balance factor $\left(F_1 F_2'\right)$

Subscripts

O, A, B, C, D, E, F, G, denote overhang-nose type (table I)

and

$$c_{L_\alpha} = \left(\frac{\partial c_L}{\partial \alpha}\right)_{\delta_f}$$

$$c_{l_\alpha} = \left(\frac{\partial c_l}{\partial \alpha}\right)_{\delta_f}$$

$$c_{L_{1_\alpha}} = \left(\frac{\partial c_{L_1}}{\partial \alpha}\right)_{\delta_f}$$

$$c_{l_{1_\alpha}} = \left(\frac{\partial c_{l_1}}{\partial \alpha}\right)_{\delta_f}$$

$$c_{l_\delta} = \left(\frac{\partial c_l}{\partial \delta_f}\right)_\alpha$$

$$c_{l_{l_\delta}} = \left(\frac{\partial c_{l_1}}{\partial \delta_f}\right)_\alpha$$

$$c_{h_\alpha} = \left(\frac{\partial C_h}{\partial \alpha}\right)_{\delta_f}$$

$$c_{h_\alpha} = \left(\frac{\partial c_h}{\partial \alpha}\right)_{\delta_f}$$

$$c_{h_\delta} = \left(\frac{\partial C_h}{\partial \delta_f}\right)_\alpha$$

$$c_{h_\delta} = \left(\frac{\partial c_h}{\partial \delta_f}\right)_\alpha$$

k lift-effectiveness parameter $\left(\dfrac{c_{l_\delta}}{c_{l_\alpha}}\right)$

k_o lift-effectiveness parameter for plain sealed

         flaps $\left(\dfrac{c_{l_{1_\delta}}}{c_{l_{1_\alpha}}}\right)$

       The subscripts outside the parentheses indicate the factors held constant during measurement of the parameters.

$\left.\begin{array}{l}\Delta C_{h_\alpha} \\ \Delta c_{h_\alpha} \\ \Delta C_{h_\delta} \\ \Delta c_{h_\delta}\end{array}\right\}$ increments of slopes of hinge-moment curves due to overhang type of balance for test conditions using data for plain unbalanced control surface with same gap condition as a base

AVAILABLE DATA

The data used in the summary were obtained from the results of model tests presented in references 7 to 24 and also from various unpublished test results. Some of the more pertinent information regarding the geometric characteristics of the models and the test conditions are summarized in table II.

Although an appreciable amount of data from tests of two-dimensional control surfaces and finite-span ailerons were available, the amount of data obtained for finite-span tail surfaces was not considered adequate for a reliable correlation.

The values of the slopes of the hinge-moment curves used in the analysis are the slopes for small control deflections at an angle of attack of $0°$.

CORRELATION METHODS

The present paper is concerned with the generalization of the effects of plain-overhang and Frise balances in providing aerodynamic balance for flap-type control surfaces. Empirical factors and design charts were desired in order that approximate relations could be established between the geometric constants of overhang balances and the effects of overhang balances on the hinge-moment slopes. A preliminary study of the problem, indicated that the slope increments ΔC_{h_δ} and ΔC_{h_α} (or Δc_{h_δ} and Δc_{h_α}) due to the overhang were more suitable for correlation than the total values of the slopes.

The aerodynamic balancing effect of an overhang balance is considered to be a maximum when the contour of the balance conforms to the contour of the airfoil for the entire length of the overhang. Rounding or tapering the nose causes a reduction in the effect of the balance. In the present analysis, the effects of overhang length and nose shape were evaluated independently by means of various cross plots of the available data. The effects of variations in the nose shape were found to depend on the overhang length; therefore, a measure

of the net balancing effect of plain-overhang or Frise
balances was obtained as a product rather than as a dif-
ference of two empirical factors. The two factors
are F_1, which is related to the length of overhang,
and F_2', which is related to the sectional shape of
the balance nose. Thus

$$K_1 = F_1 F_2'$$

where

$$F_1 = \left[\left(\frac{\overline{c}_b}{\overline{c}_f} \right)^2 - \left(\frac{\overline{t/2}}{\overline{c}_f} \right)^2 \right] \frac{b_b}{b_f}$$

and the expression for F_2' is given in table I for
various general types of nose shape. As may be seen
from table I, the expression for F_2' is, in general,
the product of an area-moment ratio and a basic nose-
shape factor that specifies the relative location of the
point of tangency of a circular-arc nose and the airfoil
contour. This basic nose-shape factor F_2 is defined
as

$$F_2 = 1 - \sqrt{1 - \left(\frac{1 + \frac{\overline{c}_b{}'}{\overline{c}_f}}{1 + \frac{\overline{c}_b}{\overline{c}_f}} \right)^2}$$

It should be noted that for any overhang having a
nose formed by circular arcs (nose types C, A, B, D, and
G of table I)

$$F_2' = F_2$$

and therefore

$$K_1 = F_1 F_2$$

If the nose shape is elliptical (type C, table I) or sharp (type E or F, table I) the factor F_2' is obtained by multiplying a nominal value of F_2 by an area-moment factor. For an elliptical nose (type C) the nominal value of F_2 is the value that would be obtained for a flap having the same overhang as the given flap but with a nose shape of type B. The appropriate area-moment factor is given in table I where M_0, M_B, and M_C are the area moments about the hinge axis of the balance profiles having nose types denoted by the subscript letters. A similar method is used for the sharp-nose balances (E and F). In these cases, the nominal value of F_2 is obtained for a circular-arc nose (type D) having a radius R_D such that the arc becomes tangent to the airfoil contour at a point defined by the intersection of the airfoil contour and an extension of the straight line forming the forward portion of the balance nose. The exponents of the area-moment factors were determined empirically.

Graphical solutions of the expressions for the overhang factor F_1 (for overhangs having spans equal to the control-surface span) and the basic nose-shape factor F_2 are presented in figure 1. The value of F_1 for balances which do not extend over the entire span of the control surface (as for conventional rudders) is obtained by multiplying the value of F_1 obtained from figure 1 by the ratio of balance span to control-surface span. The use of this figure should allow a rapid determination of F_1 and F_2, provided the geometric constants $\overline{c}_b$, $\overline{c}_b'$, $\overline{t}$, and $\overline{c}_f$ are known.

The analysis of the available data on control surfaces with beveled trailing edges (reference 4) indicated that the effects of plan form of the wing or tail surface could be accounted for reasonably well by assuming that both the lift-curve slope and the increments of hinge-moment slopes due to aerodynamic balance are affected by plan-form changes in the same manner. The same assumption has been made in the present correlation of the variation of hinge moments with control deflection.

In the original reports of the partial-span model tests (models X, XVIII, and XIX of table II) plan-form corrections were not applied to the hinge-moment data

but were applied to the other aerodynamic characteristics.
The lift characteristics used for these three models in
this correlation are those corresponding to the actual
portion of the model tested and are not the same as pre-
viously presented lift characteristics.

RESULTS

Hinge-Moment Parameters

The effects of overhang balances on the variation
of hinge-moment coefficient with control deflection are
shown in figure 2 as curves of $\Delta C_{h_\delta}/C_{L_{l_\alpha}}$ or $\Delta c_{h_\delta}/c_{l_{l_\alpha}}$

plotted against the balance factor K_1. The parame-
ter $C_{L_{l_\alpha}}$ is the average value of the lift-curve slope

over the span of the control surface and is generally
somewhat different from the lift-curve slope of the
entire wing. A method of estimating the value of $C_{L_{l_\alpha}}$

for ailerons on wings of various plan forms is given in
reference 4. For conventional tail surfaces, $C_{L_{l_\alpha}}$

generally may be assumed equal to the lift-curve slope
of the entire surface. As shown by figure 2, the varia-
tion of the parameter $\Delta C_{h_\delta}/C_{L_{l_\alpha}}$ with K_1 for finite-

span ailerons was the same as the variation of $\Delta c_{h_\delta}/c_{l_{l_\alpha}}$

with K_1 for two-dimensional flaps. The relation was
somewhat different, however, for finite-span tail surfaces
from that for finite-span ailerons or two-dimensional
flaps. No attempt has been made to account for the dif-
ference, but the assumption that hinge-moment slope
increments and the lift-curve slope vary in the same
manner with plan form is probably not valid for the very
low aspect ratios normally used for tail surfaces. The
relation indicated for finite-span tail surfaces is based
on test results of relatively few models and cannot
therefore be considered as reliable as the relation shown
for finite-span ailerons and two-dimensional flaps.

Values of $\Delta C_{h_\delta}/C_{L_{l_\alpha}}$ and $\Delta c_{h_\delta}/c_{l_{l_\alpha}}$ (for negative deflections only) for ailerons and flaps having Frise balances had essentially the same relation to the balance factor K_1 as did the values for ailerons and flaps having plain-overhang balances. The Frise data are presented in a separate plot, however, in order to show the limits of K_1 covered by the available data.

First-approximation values of $\bar{c}_b/\bar{c}_f$ required for given values of K_1 may be obtained for nose shapes of types A, B, or D from figure 3. This figure was derived from the ordinates of NACA conventional airfoils as given in reference 25, and values of $\bar{c}_b/\bar{c}_f$ obtained from this figure may be accepted as the final values for any airfoil of the NACA conventional four-digit or five-digit series. For other airfoils, figure 3 should be used only for determining first-approximation values of $\bar{c}_b/\bar{c}_f$. By use of figure 1 and one or two additional approximations the final values may be obtained.

No factor was obtained that would adequately account for all the variables which effect the variation of hinge-moment coefficient with angle of attack. The variations of ΔC_{h_α} and Δc_{h_α} with the overhang factor F_1 are presented in figure 4 for representative models having various nose shapes and open or sealed gaps. As may be seen from figure 4 ΔC_{h_α} or Δc_{h_α} increases with overhang, but the increase is less rapid for medium noses (type C) or sharp noses (type F) than for blunt noses (type B). The effect of nose shape is much greater when the gap is open than when the gap is sealed and sealing the gap generally results in a decrease in ΔC_{h_α} or Δc_{h_α} for a given balance. Little consistency in the magnitude of the decrease can be noted from figure 4.

Deflection Range

Attempts to correlate δ_{cr}, the deflection at which the overhang loses its balancing effect, with the balance factor K_1 gave unsatisfactory results. A somewhat

better correlation was obtained with the function $\dfrac{F_2{}'\sqrt{F_1}}{(1-\imath^2)}$

in which the factor $1-\imath^2$ serves to account for the lower values of δ_{cr} obtained for low-drag airfoils. The scatter of points in figure 5, which presents the correlation of δ_{cr} for $\alpha = 0^\circ$, is probably still too great to justify use of the given relation in original design work. The given relation, however, should allow satisfactory estimates of the change in δ_{cr} that might be expected to accompany minor modifications to the overhang or nose shape of balances already in use.

Lift Effectiveness

Several investigations have indicated that the lift effectiveness of a flap is a function of the overhang balance and the gap. Reasonably consistent variations of the effectiveness ratio k/k_o with the balance factor K_1 were obtained and are presented in figure 6 for several different gaps. The test values plotted are principally for 30-percent-chord flaps (only a few points for 20-percent-chord flaps were available) but the relations shown in figure 6 are believed to apply reasonably well within the limits of chord ratios normally used for control surfaces. The effectiveness parameter k for a flap having a given gap and balance factor K_1 may be determined by multiplying the value of k/k_o obtained from figure 6 by the effectiveness parameter k_o for a plain sealed flap having the same chord ratio c_f/c. That the effectiveness parameter k increases with the balance factor K_1 and that the rate of increase is greater for the larger gaps may be seen from figure 6. If the four curves of figure 6 had been plotted from the same base, they would intersect near $k/k_o = 1.05$ where $K_1 = 0.05$. Thus, for K_1 values greater than 0.05, opening a gap will generally increase k, and for K_1 values less than 0.05, opening a gap will generally decrease k. Although the lift effectiveness increases as the amount of balance increases, the unstalled deflection range decreases (fig. 5). The maximum increment of lift of a highly balanced control surface is generally somewhat less than the maximum increment of lift of the corresponding unbalanced control surface.

Effect of Gap

The effect of gap on the section hinge-moment parameters and on the critical deflection is given for a few representative two-dimensional models in figure 7. For the conventional airfoils for which results are shown there was a tendency for the values of c_{h_α} and c_{h_δ} to become less negative as the gap was increased. For the low-drag airfoil (model II), however, the values of c_{h_α} and c_{h_δ} became more negative as the gap was increased. The variations noted for the various airfoils are in agreement with the statement in reference 4 that opening a gap increases the tendency of larger trailing-edge angles to make the hinge-moment parameters more positive.

The magnitude of the critical deflection decreased with gap for the two models shown in figure 7. The rate of decrease of δ_{cr} was greater for the low-drag airfoil (model II) than for the conventional airfoil (model I).

Effect of Mach Number and Reynolds Number

The effect of a simultaneous increase in Mach number and Reynolds number on the hinge-moment parameters, the lift-effectiveness parameter, and the critical deflection is shown for three representative models in figure 8. The data are too scarce and the variations too irregular to justify any generalizations except with regard to the critical deflection, which decreased as the Mach number increased for all three cases. The variation of δ_{cr} with M was slightly greater for flaps with sealed gaps than for flaps with open gaps.

The tendency for c_{h_α} and c_{h_δ} to become less negative at the higher Mach numbers as noted for some airfoils is important because it may lead to control-force overbalance at high speed. The available data are too meager, however, to warrant rating the various airfoils and types of overhang on this basis.

Pressure Distributions

Data on the pressure distributions over control surfaces with plain-overhang and Frise balances are relatively scarce but a few sample diagrams from references 1, 19, and 26 are presented in figures 9 to 13. Additional data may be obtained from references 27 and 28.

The effects of nose radius, gap, and control-surface deflection on the pressures over control surfaces with plain-overhang balances is shown for a two-dimensional model in figure 9 and for a finite-span model in figure 10. Within the unstalled range, decreasing the nose radii had little effect on the pressures back of the hinge but increased the peak pressure at the protruding nose of the balance. Control surfaces with very small nose radii stalled at relatively low deflections. Sealing the gap decreased the positive pressures on the upper surface of the balance for negative deflections but had a negligible effect on the pressures over other portions of the control surface.

The effect of Mach number on the pressure distribution over a control surface with plain-overhang balance is shown in figure 11 for control-surface deflections of $\pm 10°$. The increase in peak negative pressure, which usually accompanies an increase in Mach number, is not evident in figure 11. Evidently the adverse pressure gradient back of the balance nose was so great that the control surface stalled at some intermediate Mach number. Pressure surveys over the lower surface at the nose and the upper surface at the hinge line of a Frise aileron on a semispan model of a low-drag wing are shown in figure 12.

The effects of nose radius, vent gap, and modifications to the slot-entry shape are shown in figure 13 for a control surface with a Frise balance. Decreasing the nose radius with this control had effects similar to those noted previously for the plain-overhang control; that is, the peak negative pressures were increased for every case except for the smallest nose radius, with which the nose was stalled at the deflection for which the diagram is shown. Increasing the vent gap or rounding the slot entry slightly reduced the negative pressures over the balance nose for negative deflections and the positive pressures over the balance nose for positive deflections. Rounding the slot entry and

increasing the vent gap increased the flow velocity
through the slot, as is evidenced by the more negative
pressures over the upper surfaces of the balance and of
the control at positive deflections.

OPTIMUM BALANCE ARRANGEMENTS

Many factors must be considered in selecting the
optimum overhang-balance arrangement for a given control
surface. The following is a brief discussion of some of
these factors.

A given value of ΔC_{h_δ} may be obtained by many va-
riations of balance length and nose shape ranging from
rather short and blunt balances to longer balances with
sharp noses. Although the geometric characteristics may
be adjusted over quite a wide range for any given value
of ΔC_{h_δ}, other aerodynamic characteristics will not

remain constant and, consequently, must be considered.

The fact that δ_{cr} varies approximately as $F_2{}'\sqrt{F_1}$,
whereas ΔC_{h_δ} varies as $F_2{}'F_1$, indicates that a long

overhang and a moderate nose shape of type B, C, or D is
more satisfactory than a short overhang and a blunt-nose
shape of type A.

A factor that is probably quite closely related
to δ_{cr} is the magnitude of the peak pressures over the
balance nose. If ΔC_{h_δ} is assumed to remain the same,

a short blunt-nose balance produces higher peak pressures
than a long balance with a moderate nose shape. The high
peak pressure associated with the very blunt nose shape
increases the possibility that the control surface may
become overbalanced at high Mach numbers and probably in-
creases the rate at which Mach number reduces the value
of δ_{cr}. The high peak pressures increase the possi-
bility that supercritical local velocities will be
reached over the nose of the balance. Although little
definite information is at present available concerning
the effects of shock waves that occur over only a rela-
tively short chordwise portion of the airfoil, such
effects are probably not beneficial.

The ease with which static balance may be obtained is important, especially for large airplanes. The long overhangs permit static balance to be obtained by the addition of a minimum of otherwise nonuseful weight.

Other considerations impose limitations on the most desirable length of overhang. A long overhang requires a large part of the fixed structure of the wing or tail surface to be cut away to allow for free movement of the balance. The large breaks in the airfoil surface that result from the use of medium or sharp nose shapes probably increase the drag.

Nose shapes of types C, D, E, or F are likely to give overbalance at high deflections if designed for slight underbalance at low deflections because a large portion of the balancing action of the overhang type of balance is produced by the negative pressure developed at the portion of the nose that protrudes above or below the airfoil contour. For nose types C and D the negative pressure peak moves forward and increases in magnitude as the deflection is increased, thereby resulting in an effective increase in balance. From these considerations it might be mentioned that a shape of type D can be expected to be more satisfactory than a shape of type C, unless the deflection limits allow the most forward point of the nose to protrude outside the airfoil contour. All the pointed nose shapes (types D, E, and F) show a greatly increased balancing effect when the nose protrudes above or below the airfoil contour. It appears that such a condition should be avoided by the use of stops unless the control deflection required would be beyond the critical value and it is desired to use the control in this condition. Control surfaces with blunt-nose overhangs (types A and B) have also shown some tendency toward increased balance at high deflections (references 7 and 19) but the effect is not as great as for the medium- and sharp-nose shapes just discussed.

As pointed out in a previous section the parameter ΔC_{h_α} is relatively independent of nose shape for sealed balances and appears to depend principally on the balance chord. The choice of the best combination of nose shape and overhang for a given ΔC_{h_δ} may therefore be influenced by the value of ΔC_{h_α} obtained, the degree of influence depending on the specific application.

The choice of an open or a sealed gap for use with the overhang will be influenced by the fact that nose shape has more effect on C_{h_α} with the gap open than with the gap sealed. For balances having values of K_1 greater than about 0.05 the use of an open gap generally increases the lift-effectiveness parameter k of the control surface. Part of the gain in k, however, is obtained at the expense of a loss in c_{l_α}. The loss in c_{l_α} generally is not harmful if the control surface is an aileron but affects the airplane stability adversely if the control surface is a rudder or an elevator.

The possibility of any buffeting tendency should not be overlooked in the design of a balanced control surface. Flight tests as well as wind-tunnel tests have revealed such tendencies for Frise ailerons as pointed out in reference 1. The buffeting appears to occur in the region of the negative deflections at which the air flow separates from the protruding nose; that is, at deflections near the critical values given for zero angle of attack in figure 5. An increase in angle of attack usually delays buffeting for Frise ailerons. Buffeting may also be delayed by any modification that tends to delay separation; that is, by increasing the nose radius, reducing the overhang, raising the nose, bulging the lower surface of the aileron, or providing the nose with a slot or a slat. With the possible exception of the addition of a slot or slat, all these measures tend to reduce the aerodynamic balance for small deflections.

Some buffeting was noted during tests of two models having plain-overhang balances. The oscillations were not so severe, however, as those noted for Frise balances. Because this type of balance may protrude into the air stream either above or below the airfoil surface, the deflection at which buffeting may occur would be expected to be less for either positive or negative angles of attack than for zero angle of attack.

From the foregoing discussion it may be concluded that the final selection of a control-surface nose shape must be a compromise depending on the relative importance of the various factors considered.

In the case of ailerons, the selection of overhang and nose shape may be made principally from a consideration of the value of C_{h_δ} required. The effect of C_{h_α} on the stick forces during a roll must be considered in the choice of C_{h_δ}, but the adjustment of the nose shape or overhang of ailerons to obtain a desired value of C_{h_α} is not recommended. A nose shape similar to type B seems the most promising of those tested; therefore, for original design work, it should generally be necessary to determine only the overhang for a nose shape of type B required to give a value of C_{h_δ} already decided upon. The value of C_{h_δ} actually obtained may be adjusted later within a limited range by making minor modifications to the nose shape without changing the length of overhang. The effect of nose shape on the peak pressures, the critical deflection, and the variation of C_{h_δ} with deflection, however, must be given consideration.

The hinge-moment parameters C_{h_δ} and C_{h_α} are of almost equal importance for tail surfaces, and the selection of the overhang and nose shape therefore depends on obtaining desirable values for each of these parameters. As has already been pointed out, the nose shape has little effect on C_{h_α} provided the gap is sealed. The overhang may consequently be selected to obtain the desired value of C_{h_α} and the nose shape may then be selected to obtain the desired value of C_{h_δ}, due consideration being taken of the effect of nose shape on the peak pressure, on the critical deflection, and on the variation of C_{h_δ} with deflection. If the desired value of C_{h_δ} cannot be obtained by selection of only the nose shape, some adjustment of the overhang may be necessary, and compromise values of C_{h_δ} and C_{h_α} will thereby be obtained.

COMPARISON OF RESULTS WITH THEORY

The faired curve of figure 2(b) and the theoretical values of c_{h_δ} for plain sealed flaps derived by Glauert and presented in references 29 and 30 were used in computing the hinge moments of flaps with plain sealed overhangs on an infinitely thin airfoil, for which K_1 reduces to $(c_b/c_f)^2$. The values thus computed were then compared with theoretically derived values presented in figure 5 of reference 31. The data of reference 31 are presented for values of the over-all control-surface chord $(c_b + c_f)$ equal to 0.25c and 0.50c with various hinge locations for several values of a parameter λ. In reference 31, λ is an effective reduction in balance chord and is the distance over which the concentrated source-sink representing the steep break at the balance nose is spread in order to picture the local flow and at the same time retain physical reality. According to reference 31, λ is probably greater than 5 percent and less than 40 percent of the balance chord for airfoils of finite thickness. The values for an infinitely thin airfoil would be expected to fall near the lower limit of the suggested range of λ. This premise is borne out by a comparison of the theoretical curves and the experimental data extrapolated to zero thickness in the manner noted. The experimental data forms a curve located at $\lambda = 0.03$ to 0.05 for both values of over-all control surface chord.

DESIGN PROCEDURE

The results of the present analysis are considered applicable to the original design of control-surface balances and of balance modifications for control surfaces already in use. The procedure recommended for an original design will be illustrated in detail by an example:

Let it be required to estimate the length of plain overhang for a nose shape of type B to give a final value of C_{h_δ} of -0.0010 for a 0.20c aileron on an NACA 23012 airfoil. The aerodynamic characteristics needed in the design are: (1) the slope C_{h_δ} of the

plain unbalanced aileron having the same gap condition
as the proposed balanced aileron, and (2) the average
slope of the lift curve over the aileron portion of the
wing $C_{L_{1_\alpha}}$

Because only the increments of slopes due to the
balance are considered in the present correlation of
hinge-moment characteristics, the ability to obtain a
desired value of C_{h_δ} for the balanced control surface

is critically dependent upon the accuracy of the value
of C_{h_δ} used as a base. The value of this base may be
estimated from comparable finite-span data or calculated
from section data, but the final value of C_{h_δ} obtained

for the balanced aileron cannot be expected to be more
accurate than the value used for the base. The slope of
the lift curve of the entire surface C_{L_α} will usually

be known from experimental data. The average slope over
the span of the aileron $C_{L_{1_\alpha}}$ may be estimated with suf-

ficient accuracy by the method of reference 4.

It is assumed that the following results were ob-
tained:

C_{h_δ} (for plain unbalanced aileron) = -0.0070

$$C_{L_{1_\alpha}} = 0.080$$

The increment of hinge-moment slope required of the
plain-overhang balance is

$$\Delta C_{h_\delta} = -0.0010 - (-0.0070) = 0.0060$$

and therefore

$$\frac{\Delta C_{h_\delta}}{C_{L_{1_\alpha}}} = \frac{0.0060}{0.080} = 0.075$$

For finite-span ailerons the balance factor K_1 is equal

to $\dfrac{\Delta C_{h_\delta}}{C_{L_{1_\alpha}}}$ (fig. 2); thus,

$$K_1 = 0.075$$

The required overhang for a nose shape of type B may now be determined approximately from figure 3(a), by use of the value of K_1 just determined and $\dfrac{t/2}{c_f} = 0.131$ from the known airfoil ordinates at the aileron hinge line. Therefore,

$$\frac{\overline{c}_b}{\overline{c}_f} = 0.397$$

The accuracy of this value may be checked by drawing the aileron nose to the proper ordinates (balance 1 of fig. 14) from which the contour-balance chord may be obtained graphically. For constant-percentage-chord ailerons, the result is

$$\frac{\overline{c}_b{}'}{\overline{c}_f} = 0.221$$

Now, from figure 1, $F_1 = 0.141$, $F_2 = 0.521$, and therefore $K_1 = 0.074$, which is sufficiently close to the value required. As has already been shown, the value of $\overline{c}_b/\overline{c}_f$ obtained from figure 3 may be accepted as the final value for nose shapes of type A, B, or D for any airfoil of the NACA conventional four-digit or five-digit series and, therefore, the check just performed was not necessary in this instance. If an airfoil section having a different thickness distribution had been used, or if it had been desired to use a nose shape other than type A, B, or D, figure 3 would still have been used, but only to obtain a preliminary estimate of $\overline{c}_b/\overline{c}_f$.

The procedure to be used in connection with proposed modifications to plain-overhang balances is similar to that just outlined for an original design except that the value of C_{h_δ} of the original balanced control surface may be used as the base. If only a certain increment ΔC_{h_δ} is desired, no base value is necessary.

In order to illustrate the change in overhang that would normally be required to give the same amount of aerodynamic balance for small deflections when the nose radii are varied, two additional nose shapes have been derived and are presented in figure 14(a). Balance 2 has one and one-half times the nose radius of balance 1 and balance 3 has one half the nose radius of balance 1. The geometric constants of the three balances are tabulated in figure 14(a).

The variation of C_{h_δ} that may be expected to accompany moderate changes in the nose radius with a fixed overhang is indicated in figure 14(b). The estimated values of C_{h_δ} range from -0.0022 to 0.0002.

The recommended procedure for the design or modification of control surfaces with Frise balances is similar to that just outlined for plain-overhang balances except that the increment ΔC_{h_δ} applies only to the negative deflection range. The slope C_{h_δ} for positive deflections greater than about 8° may be considered to be unaffected by overhang or nose shape. The complete hinge-moment curve can be approximated with a fair degree of accuracy at low angles of attack by fairing a curve between the balanced negative portion (tangent at $\delta_f \approx -2^\circ$) and the unbalanced positive portion (tangent at $\delta_f \approx 8^\circ$). The exact location of the curve with respect to the axes is dependent on a number of factors, however, including the shape of the airfoil section. A prediction of the characteristics of a control surface with a Frise balance, therefore, cannot be expected to be as accurate as a prediction for a control surface with a plain-overhang balance. It is believed, however, that the effect of minor modifications to either plain-overhang or Frise balances can be predicted with fair accuracy by the method outlined.

CONCLUSIONS

The results of the preceding correlation and analysis indicate the following general conclusions regarding control surfaces having plain-overhang or Frise balances:

1.   The effects of balance variations in changing the slope of the curve of hinge-moment coefficient plotted against control-surface deflection and in changing the lift effectiveness of the control surface could be correlated for various models at low Mach numbers by the use of a balance factor that accounted for the size and shape of the overhang.

2.   No correlation factor was obtained that would adequately account for all the variables which affect the slope of the curve of hinge-moment coefficient plotted against angle of attack or which affect the deflection range over which the balance is effective in reducing the slope of the hinge-moment curve.

3.   The presence of a small gap at the nose of a plain-overhang balanced flap and of the corresponding unbalanced flap does not appreciably alter the differences in the slopes of the curves of hinge moment plotted against control deflection.

4.   The shape of the balance nose varied the effect of a gap at the control leading edge on the slope of the curve of hinge moment plotted against angle of attack for plain-overhang balances.

5.   The presence of a gap at the control leading edge consistently increased the effect of overhang in increasing the control lift-effectiveness parameter. With the open gap the increase in the lift-effectiveness parameter with increase in overhang was caused by an increase in the slope of the curve of lift plotted against control-surface deflection and a decrease in the slope of the curve of lift plotted against angle of attack.

6. The data were too meager to justify any definite generalizations concerning the effects of Mach number on plain-overhang and Frise balances except that increases in Mach number consistently decreased the deflection range over which the balance was effective in reducing the slope of the hinge-moment curve.

Langley Memorial Aeronautical Laboratory,
        National Advisory Committee for Aeronautics,
            Langley Field, Va.,

REFERENCES

1. Rogallo, F. M.: Collection of Balanced-Aileron
        Test Data. NACA ACR No. 4A11, 1944.

2. Sears, Richard I.: Wind-Tunnel Data on the Aero-
        dynamic Characteristics of Airplane Control
        Surfaces. NACA ACR No. 3L08, 1943.

3. Rogallo, F. M., and Lowry, John G.: Résumé of Data
        for Internally Balanced Ailerons. NACA RB,
        March 1943.

4. Purser, Paul E., and Gillis, Clarence L.: Prelimi-
        nary Correlation of the Effects of Beveled
        Trailing Edges on the Hinge-Moment Characteristics
        of Control Surfaces. NACA CB No. 3E14, 1943.

5. Lowry, John G.: Résumé of Hinge-Moment Data for
        Unshielded Horn-Balanced Control Surfaces. NACA
        RB No. 3F19, 1943.

6. Jacobs, Eastman N., Abbott, Ira H., and Davidson,
        Milton: Supplement (loose-leaf) to NACA Advance
        Confidential Report, Preliminary Low-Drag-Airfoil
        and Flap Data from Tests at Large Reynolds Numbers
        and Low Turbulence. NACA, March 1942, p. 21a.

7. Letko, W., Hollingworth, T. A., and Anderson, R. A.:
        Wind-Tunnel Tests of Ailerons at Various Speeds.
        IV - Ailerons of 0.20 Airfoil Chord and True
        Contour with 0.35 Aileron-Chord Extreme Blunt-
        Nose Balance on the NACA 23012 Airfoil. NACA ACR
        No. 3H28, 1943.

8. Letko, W., Denaci, H. G., and Freed, C.: Wind-Tunnel
        Tests of Ailerons at Various Speeds. I - Ailerons
        of 0.20 Airfoil Chord and True Contour with 0.35
        Aileron-Chord Extreme Blunt Nose Balance on the
        NACA 66,2-216 Airfoil. NACA ACR No. 3F11, 1943.

9. Sears, Richard I.: Wind-Tunnel Investigation of
        Control-Surface Characteristics. I - Effect of
        Gap on the Aerodynamic Characteristics of an
        NACA 0009 Airfoil with a 30-Percent-Chord Plain
        Flap. NACA ARR, June 1941.

10. Ames, Milton B., Jr.: Wind-Tunnel Investigation of
       Control-Surface Characteristics. III - A Small
       Aerodynamic Balance of Various Nose Shapes Used
       with a 30-Percent-Chord Flap on an NACA 0009
       Airfoil. NACA ARR, Aug. 1941.

11. Ames, Milton B., Jr., and Eastman, Donald R., Jr.:
       Wind-Tunnel Investigation of Control-Surface
       Characteristics. IV - A Medium Aerodynamic
       Balance of Various Nose Shapes Used with a
       30-Percent-Chord Flap on an NACA 0009 Airfoil.
       NACA ARR, Sept. 1941.

12. Sears, Richard I., and Hoggard, H. Page, Jr.: Wind-
       Tunnel Investigation of Control-Surface Charac-
       teristics. II - A Large Aerodynamic Balance of
       Various Nose Shapes with a 30-Percent-Chord Flap
       on an NACA 0009 Airfoil. NACA ARR, Aug. 1941.

13. Gillis, Clarence L., and Lockwood, Vernard E.:
       Wind-Tunnel Investigation of Control-Surface
       Characteristics. XIII - Various Flap Overhangs
       Used with a 30-Percent-Chord Flap on an NACA
       66-009 Airfoil. NACA ACR No. 3G20, 1943.

14. Sears, Richard I., and Liddell, Robert B.: Wind-
       Tunnel Investigation of Control-Surface Charac-
       teristics. VI - A 30-Percent-Chord Plain Flap
       on the NACA 0015 Airfoil. NACA ARR, June 1942.

15. Sears, Richard I., and Hoggard, H. Page, Jr.: Wind-
       Tunnel Investigation of Control-Surface Charac-
       teristics. VII - A Medium Aerodynamic Balance of
       Two Nose Shapes Used with a 30-Percent-Chord Flap
       on an NACA 0015 Airfoil. NACA ARR, July 1942.

16. Sears, Richard I., and Gillis, Clarence L.: Wind-
       Tunnel Investigation of Control-Surface Charac-
       teristics. VIII - A Large Aerodynamic Balance
       of Two Nose Shapes Used with a 30-Percent-Chord
       Flap on an NACA 0015 Airfoil. NACA ARR, July
       1942.

17. Hoggard, H. Page, Jr.: Wind-Tunnel Investigation of
       Control-Surface Characteristics. X - A 30-Percent-
       Chord Plain Flap with Straight Contour on the
       NACA 0015 Airfoil. NACA ARR, Sept. 1942.

18. Sears, Richard I., and Hoggard, H. Page, Jr.: Wind-
    Tunnel Investigation of Control-Surface Charac-
    teristics. XI - Various Large Overhang and
    Internal-Type Aerodynamic Balances for a Straight
    Contour Flap on the NACA 0015 Airfoil. NACA ARR,
    Jan. 1943.

19. Purser, Paul E., and Toll, Thomas A.: Wind-Tunnel
    Investigation of the Characteristics of Blunt-
    Nose Ailerons on a Tapered Wing. NACA ARR,
    Feb. 1943.

20. Sears, Richard I., and Hoggard, H. Page, Jr.: Char-
    acteristics of Plain and Balanced Elevators on a
    Typical Pursuit Fuselage at Attitudes Simulating
    Normal-Flight and Spin Conditions. NACA ARR,
    March 1942.

21. Goett, Harry J., and Reeder, J. P.: Effects of
    Elevator Nose Shape, Gap, Balance, and Tabs on
    the Aerodynamic Characteristics of a Horizontal
    Tail Surface. NACA Rep. No. 675, 1939.

22. Letko, W., and Kemp, W. B.: Wind-Tunnel Tests of
    Ailerons at Various Speeds. III - Ailerons of
    0.20 Airfoil Chord and True Contour with 0.35-
    Aileron-Chord Frise Balance on the NACA 23012
    Airfoil. NACA ACR No. 3I14, 1943.

23. Holtzclaw, Ralph W., and Erickson, Myles D.: Wind-
    Tunnel Investigation of Flap, Aileron, and
    Exterior Bomb Installations on a 24-Inch Constant-
    Chord North American XB-28 Wing Model. NACA ARR,
    July 1942.

24. Rogallo, F. M., and Purser, Paul E.: Wind-Tunnel
    Investigation of 20-Percent-Chord Plain and Frise
    Ailerons on an NACA 23012 Airfoil. NACA ARR,
    Dec. 1941.

25. Jacobs, Eastman N., Pinkerton, Robert M., and
    Greenberg, Harry: Tests of Related Forward-
    Camber Airfoils in the Variable-Density Wind
    Tunnel. NACA Rep. No. 610, 1937.

26. Letko, W., and Denaci, H. G.: Wind-Tunnel Tests of
     Ailerons at Various Speeds. V - Pressure Distri-
     butions over the NACA 66,2-216 and NACA 23012
     Airfoils with Various Balances on 0.20-Chord
     Ailerons. NACA ACR No. 3K05, 1943.

27. Dingeldein, Richard C.: Full-Scale Tunnel Investi-
     gation of the Pressure Distribution over the
     Tail of the P-47B Airplane. NACA ARR No. 3E25,
     1943.

28. LeBeck, Robert K.: 20-Foot Wind Tunnel Pressure
     Distribution Measurements on the Full-Scale Tail
     Surfaces of the Republic P-47B Airplane - Test
     No. 14. AAF T.R. No. 4926, Materiel Command,
     Army Air Forces, May 13, 1943.

29. Glauert, H.: Theoretical Relationships for an
     Aerofoil with Hinged Flap. R. & M. No. 1095,
     British A.R.C., 1927.

30. Ames, Milton B., Jr., and Sears, Richard I.: Deter-
     mination of Control-Surface Characteristics from
     NACA Plain-Flap and Tab Data. NACA Rep. No. 721,
     1941.

31. Theodorsen, Theodore, and Garrick, I. E.: Non-
     stationary Flow about a Wing-Aileron-Tab Combina-
     tion Including Aerodynamic Balance. NACA Rep.
     No. 736, 1942.

TABLE I.- VARIOUS NOSE SHAPES CONSIDERED IN CORRELATION OF PLAIN-OVERHANG AND FRISE BALANCES AND CORRESPONDING EXPRESSIONS FOR NOSE-SHAPE FACTOR.

L-665

Nose type	Section showing nose shape	Nose-shape factor, F_2'
O		$1 - \sqrt{1 - \left(\dfrac{1 + \bar{c}_b'/\bar{c}_f}{1 + \bar{c}_b/\bar{c}_f}\right)^2}$
A		$1 - \sqrt{1 - \left(\dfrac{1 + \bar{c}_b'/\bar{c}_f}{1 + \bar{c}_b/\bar{c}_f}\right)^2}$
B		$1 - \sqrt{1 - \left(\dfrac{1 + \bar{c}_b'/\bar{c}_f}{1 + \bar{c}_b/\bar{c}_f}\right)^2}$
C		$\left(\dfrac{M_C - M_O}{M_B - M_O}\right)^{1.4}\left(1 - \sqrt{1 - \left(\dfrac{1 + \bar{c}_b'/\bar{c}_f}{1 + \bar{c}_b/\bar{c}_f}\right)^2}\right)$
D		$1 - \sqrt{1 - \left(\dfrac{1 + \bar{c}_b'/\bar{c}_f}{1 + \bar{c}_b/\bar{c}_f}\right)^2}$
E		$\left(\dfrac{M_E - M_O}{M_D - M_O}\right)^{0.7}\left(1 - \sqrt{1 - \left(\dfrac{1 + \bar{c}_b'/\bar{c}_f}{1 + \bar{c}_b/\bar{c}_f}\right)^2}\right)$
F		$\left(\dfrac{M_F - M_O}{M_D - M_O}\right)^{0.7}\left(1 - \sqrt{1 - \left(\dfrac{1 + \bar{c}_b'/\bar{c}_f}{1 + \bar{c}_b/\bar{c}_f}\right)^2}\right)$
G		$1 - \sqrt{1 - \left(\dfrac{1 + \bar{c}_b'/\bar{c}_f}{1 + \bar{c}_b/\bar{c}_f}\right)^2}$

NATIONAL ADVISORY
COMMITTEE FOR AERONAUTICS.

Table II.- INFORMATION REGARDING TESTS OF MODELS HAVING BALANCED CONTROL SURFACES

A - CONTROL SURFACES WITH EXPOSED-OVERHANG BALANCES

NATIONAL ADVISORY
COMMITTEE FOR AERONAUTICS.

[Designations of low-drag airfoils, regardless of the form in which they appear in the other references, are changed throughout to the form prescribed on p. 21a of reference 6]
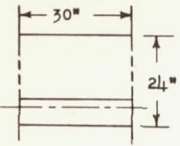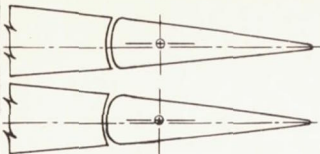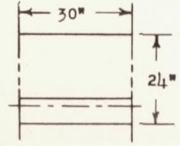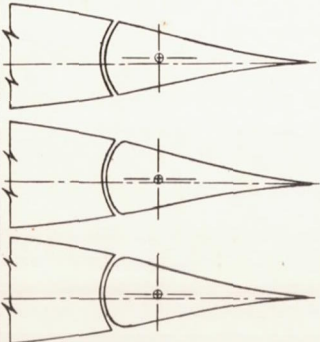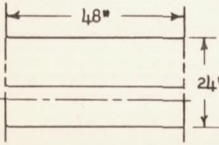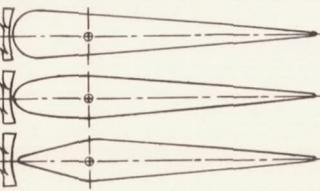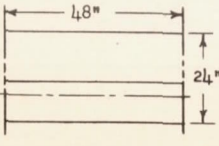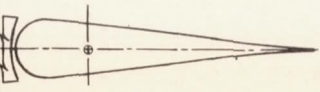
Sym-bol	Model Designation	Model Plan form of surface	Typical section of control surface	Airfoil section	A	λ	$\overline{c}_f/\overline{c}$	$\overline{c}_b/\overline{c}_f$	Gap	Type of test	Reference
⊙	I	30" 24"		NACA 23012	∞	---	0.20	0.35	Sealed 0.0005c .0030c .0055c .0107c	Two-dimensional	7
△	II	30" 24"		NACA 66(215)-216, a = 1.0	∞	---	0.20	0.35	Sealed 0.0005c .0030c .0055c .0107c	Two-dimensional	8
⊡	III	48" 24"		NACA 0009	∞	---	0.30	0.092 .200 .350 .495	Sealed 0.0010c .0015c .0050c .0100c	Two-dimensional	9, 10, 11, 12
▽	IV	48" 24"		NACA 66-009	∞	---	0.30	0.113 .350 .500	Sealed 0.005c	Two-dimensional	13

Table II.- INFORMATION REGARDING TESTS OF MODELS HAVING BALANCED CONTROL SURFACES - Continued

A - CONTROL SURFACES WITH EXPOSED-OVERHANG BALANCES - Continued

[Designations of low-drag airfoils, regardless of the form in which they appear in the other references, are changed throughout to the form prescribed on p. 21a of reference 6]

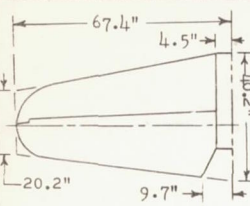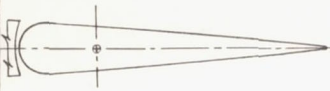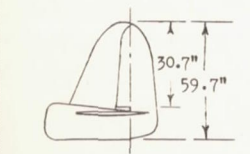NATIONAL ADVISORY
COMMITTEE FOR AERONAUTICS.

Model			Typical section of control surface	Airfoil section	A	λ	$\bar{c}_f/\bar{c}$	δ_b/δ_f	Gap	Type of test	Reference
Symbol	Designation	Plan form of surface									
◁	V	48" / 24"		Modified NACA 66-009 (straight-contour flap)	∞	---	0.26	0.30	Sealed 0.001c	Two-dimensional	----
◇	VI	48" / 24"		NACA 0015	∞	---	0.30	0.153 .350 .500	Sealed 0.005c	Two-dimensional	14, 15 16
X	VII	48" / 24"		Modified NACA 0015 (straight-contour flap)	∞	---	0.30	0.153 .500	0.005c	Two-dimensional	17, 18

Table II.- INFORMATION REGARDING TESTS OF MODELS HAVING BALANCED CONTROL SURFACES - Continued

A - CONTROL SURFACES WITH EXPOSED-OVERHANG BALANCES - Continued

[Designations of low-drag airfoils, regardless of the form in which they appear in the other references, are changed throughout to the form prescribed on p. 21a of reference 6]

NATIONAL ADVISORY COMMITTEE FOR AERONAUTICS.
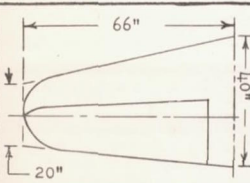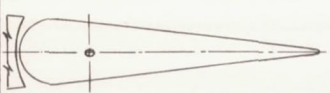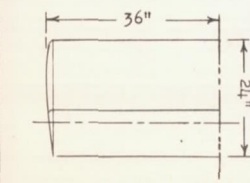
Symbol	Designation	Model — Plan form of surface	Typical section of control surface	Airfoil section	A	λ	$\overline{c}_f/\overline{c}$	$\overline{c}_b/\overline{c}_f$	Gap	Type of test	Reference
▽	VIII	18.00", 7.62", 43.20", 22.50", 45.00"		Root, NACA 23015 / Tip, NACA 4412	7.2	0.42	{0.195, .206}	{0.400, .322}	0.0025c	Complete model	---
◁	IX	90.40", B, A, 5", 5", 88.80", 52.30", 25.31", 41.55"		Root, NACA 23015.5 (approx.) / Tip, NACA 23008.25 (approx.)	5.6	0.60	0.155	{0.113, .300, .400}	{Sealed, 0.005c}	Semispan wing model	19
▷	X	178.7", Tunnel wall, 168.9, 89.3", 114.7", 45.3", 114.4		Root, NACA 65(223)-222 a = 1.0 / Tip, NACA 65(216)-415 a = 0.5	[a]12.0	[a]0.32	0.225	~0.35	0.005c	Quarter-span wing model	---
+	XI	7.15", 11.21, 2.66", 15.36", 3.0"		NACA 0009	3.7	0.57	0.30	{0.090, .350, .500}	{Sealed, 0.005c}	Tail-surface model mounted on fuselage	20

[a]Values given are for complete wing and not for partial-span wing tested.

Table II.- INFORMATION REGARDING TESTS OF MODELS HAVING BALANCED CONTROL SURFACES - Continued

A - CONTROL SURFACES WITH EXPOSED-OVERHANG BALANCES - Concluded

[Designations of low-drag airfoils, regardless of the form in which they appear in the other references, are changed throughout to the form prescribed on p. 21a of reference 6]

	Model		Typical section of control surface	Airfoil section	A	λ	$\overline{c}_f/\overline{c}$	$\overline{c}_b/\overline{c}_f$	Gap	Type of test	Reference
Symbol	Designation	Plan form of surface									
△	XII	67.4"; 4.5"; 10.2"; 20.2"; 9.7"		NACA 0009	4.7	0.50	0.45	0.10 .20	0.005c	Isolated full-scale tail surface	21
◿	XIII	30.7"; 59.7"		Modified NACA 66-series	2.41	----	0.40	0.12 .30 .50	Sealed 0.0035c	Tail-surface model mounted on stub fuselage	--
⊙	XIV	66"; 40"; 20"		Root, NACA 0015 Tip, NACA 0009	4.5	0.50	0.437 .427 .417 .461	0.364 .397 .430 .410	0.0036c	Semispan tail surface	--
◇	XV	36"; 24"		NACA 0009	3.0	1.00	0.30	0.35 .50	Sealed 0.005c	Semispan tail surface	--

NATIONAL ADVISORY
COMMITTEE FOR AERONAUTICS.

Table II.- INFORMATION REGARDING TESTS OF MODELS HAVING BALANCED CONTROL SURFACES - Concluded

B - CONTROL SURFACES WITH FRISE BALANCES

[Designations of low-drag airfoils, regardless of the form in which they appear in the other references, are changed throughout to the form prescribed on p. 21a of reference 6]

| Sym-bol | | Model | | Airfoil section | A | λ | $\overline{c}_f/\overline{c}$ | $\overline{c}_b/\overline{c}_f$ | Gap | Type of test | Refer-ence |
	Des-igna-tion	Plan form of surface	Typical section of control surface								
◌	XVI	30" 24"		NACA 23012	∞	---	0.20	0.35	0.005c	Two-dimensional	22
◌	XVII	84" 24" End Plate 42"		NACA Conventional section (approx. 14 percent thick)	∞	---	0.20	0.37	Open	Two-dimensional	23
◌	XVIII	178.7" Tunnel wall 168.9" 89.3 14.7" 114.4 45.3"		Root, 65(223)-222 a = 1.0 | Tip, 65(216)-415 a = 0.5	[a]12.0	[a]0.32	0.23	0.42	Open	Quarter-span wing model	--
◌	XIX	132.00" 123.20" 44.00" Tunnel wall 51.20" 23.20" NACA 66(215)-2(13.7,13.5) NACA 66(215)-2(13.7,16.5) 21.54"		NACA low-drag (See plan form)	[a]7.3	[a]0.42	0.20	{ 0.295 .290 .283 .400 }	Open	Third-span wing model	--
◌	XX	96" 48" 60"		NACA 23012	4.0	1.00	0.20	{ 0.278 .326 }	Open	Semispan wing model	24

[a]Values given are for complete wing and not for partial-span wing tested.

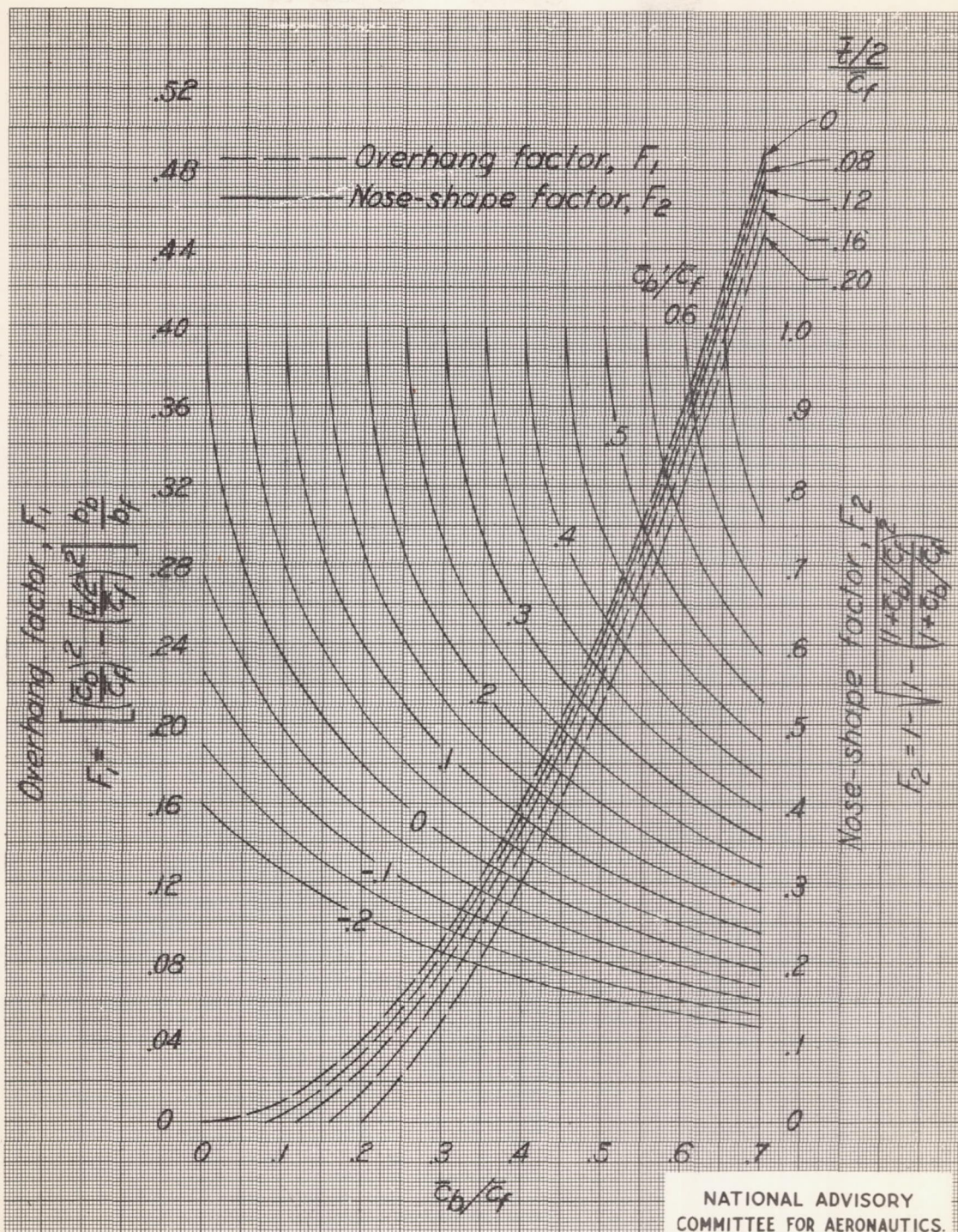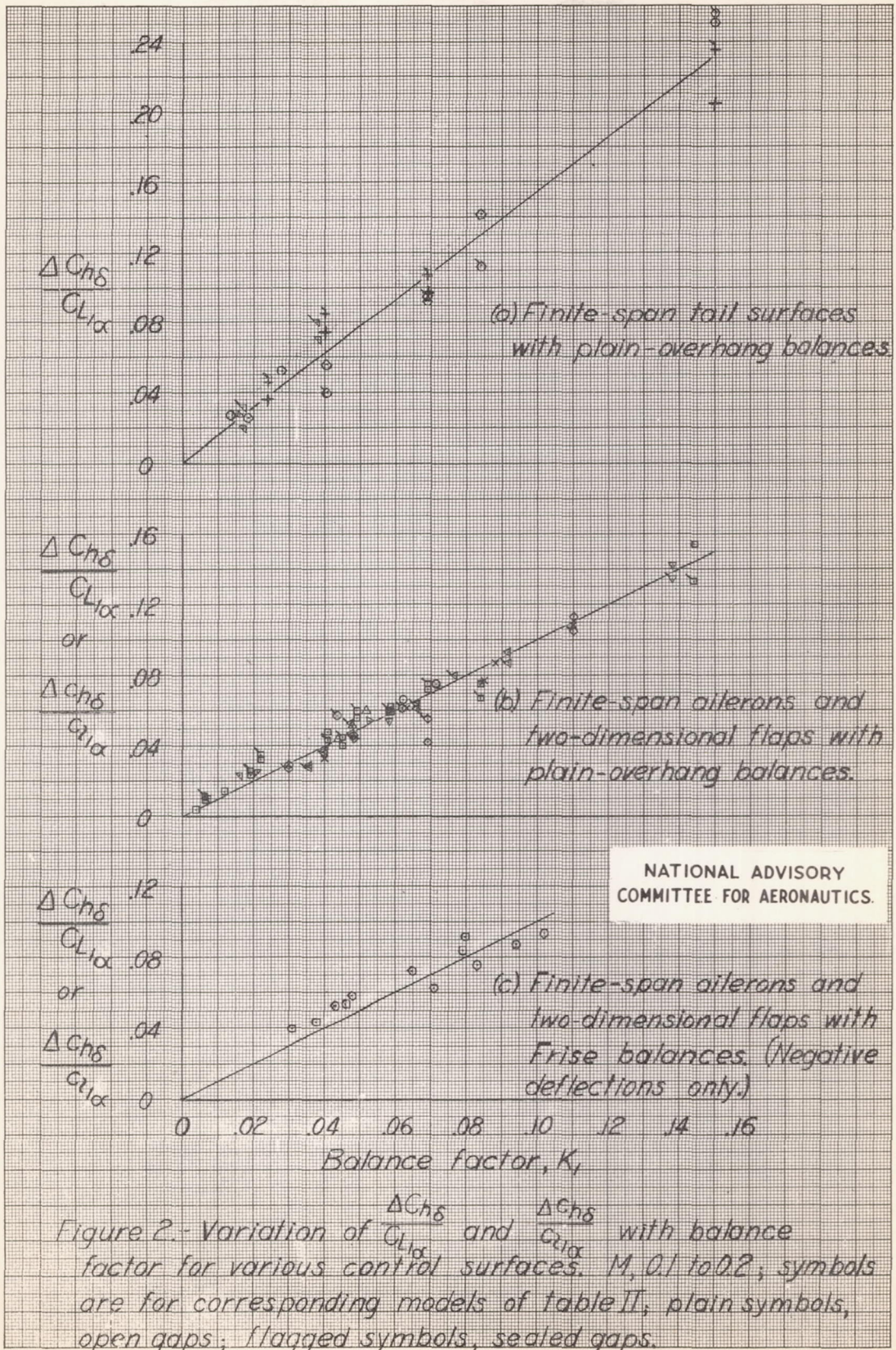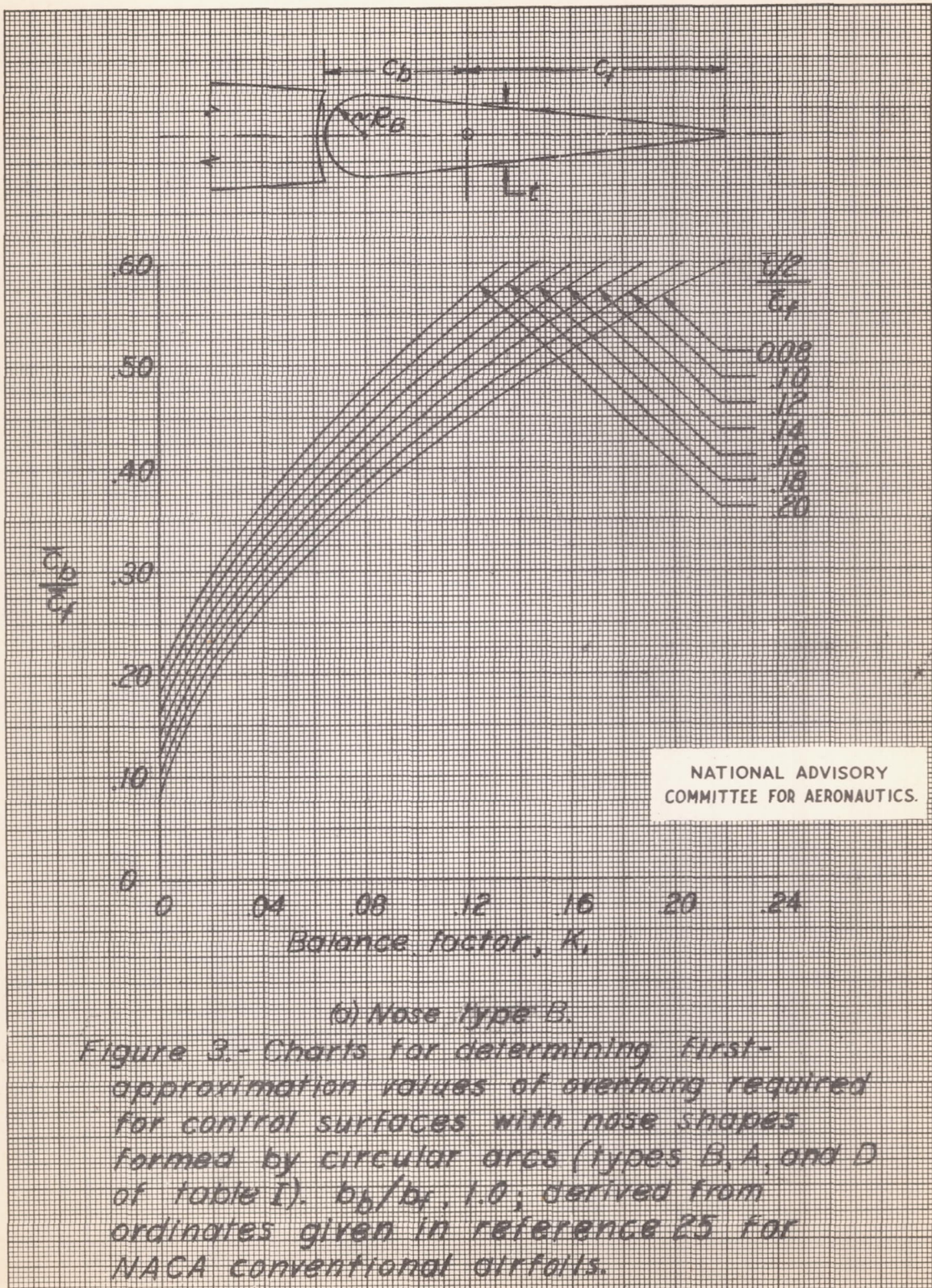NATIONAL ADVISORY
COMMITTEE FOR AERONAUTICS.

L-665

Figure 1.- Charts for determining numerical values of overhang factor and basic nose-shape factor from geometrical constants of control surfaces with plain-overhang or Frise balances. b_b/b_f, 1.0.
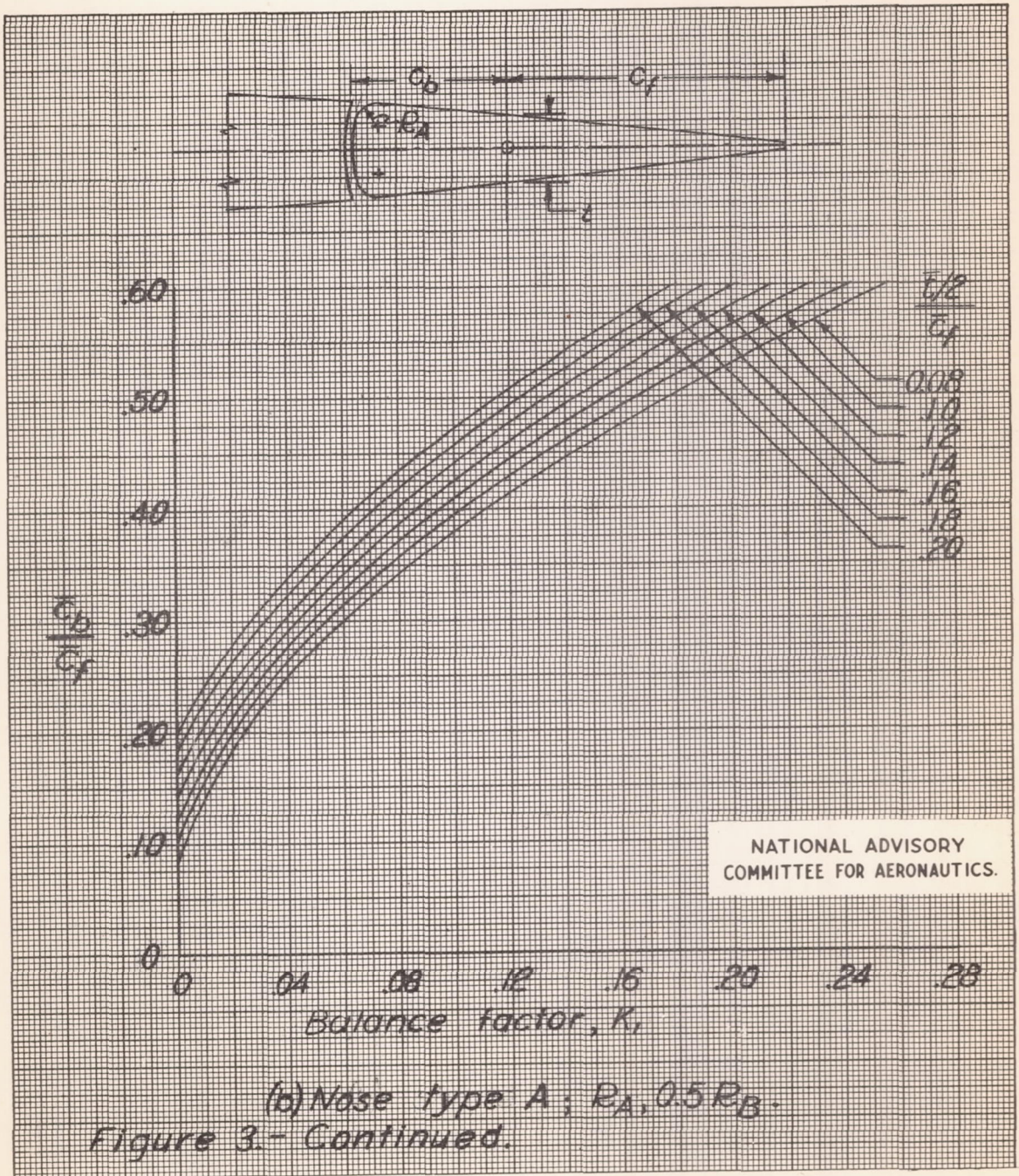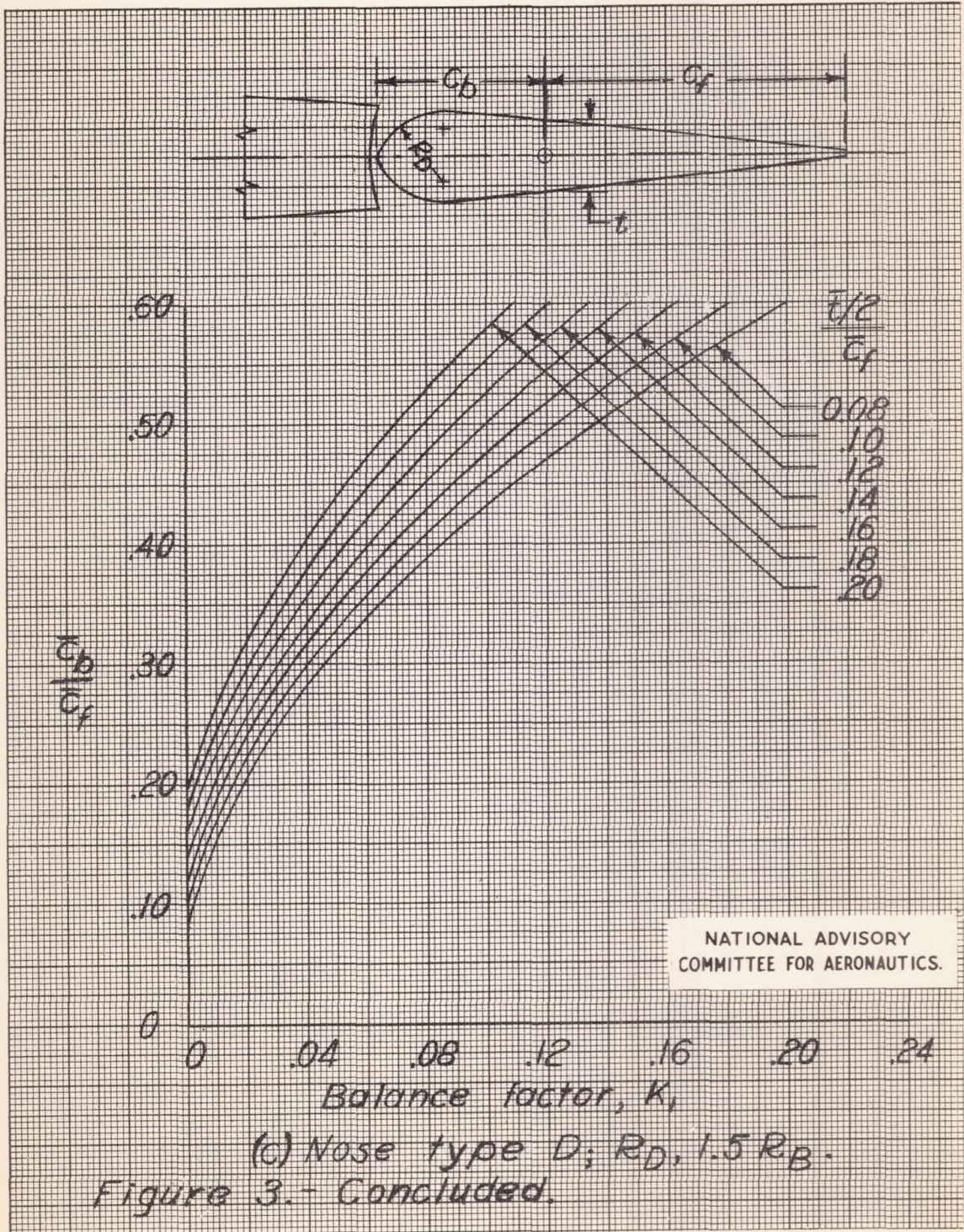
L-665

(a) Finite-span tail surfaces with plain-overhang balances.

(b) Finite-span ailerons and two-dimensional flaps with plain-overhang balances.

NATIONAL ADVISORY
COMMITTEE FOR AERONAUTICS.

(c) Finite-span ailerons and two-dimensional flaps with Frise balances. (Negative deflections only.)

Balance factor, K_1

Figure 2.- Variation of $\dfrac{\Delta C_{h\delta}}{C_{L_{l\alpha}}}$ and $\dfrac{\Delta C_{h\delta}}{c_{l_1\alpha}}$ with balance factor for various control surfaces. M, 0.1 to 0.2; symbols are for corresponding models of table II; plain symbols, open gaps; flagged symbols, sealed gaps.

(b) Nose type B.

Figure 3.- Charts for determining first-approximation values of overhang required for control surfaces with nose shapes formed by circular arcs (types B, A, and D of table I). c_b/c_f, 1.0; derived from ordinates given in reference 25 for NACA conventional airfoils.

L-665

NATIONAL ADVISORY
COMMITTEE FOR AERONAUTICS.

(b) Nose type A; R_A, 0.5 R_B.

Figure 3.- Continued.

L-665

(c) Nose type D; R_D, $1.5 R_B$.

Figure 3.- Concluded.

NATIONAL ADVISORY
COMMITTEE FOR AERONAUTICS.

Figure 4.- Variation of increment of hinge-moment slope $\Delta C_{h\alpha}$ (or $\Delta c_{h\alpha}$) with overhang factor for various balanced control surfaces. M, 0.1 to 0.2.

Fig. 4
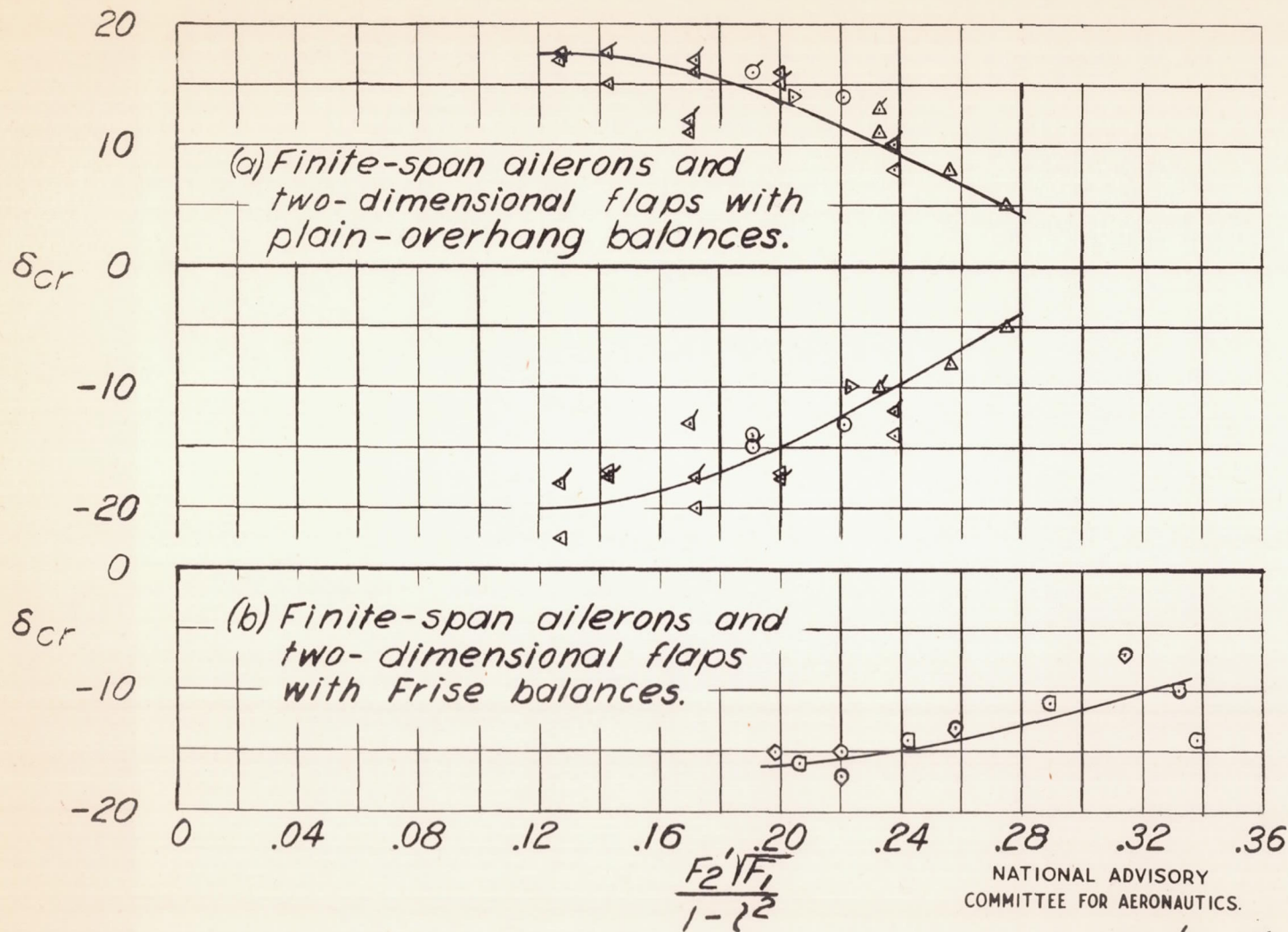
Figure 5.— Variation of critical deflection with factor $F_2'\sqrt{F_1}/(1-\zeta^2)$ for balanced control surfaces. M, 0.1 to 0.2; α, 0°; symbols are for corresponding models of table II; plain symbols, open gaps; flagged symbols, sealed gaps.

Fig. 5

L-665
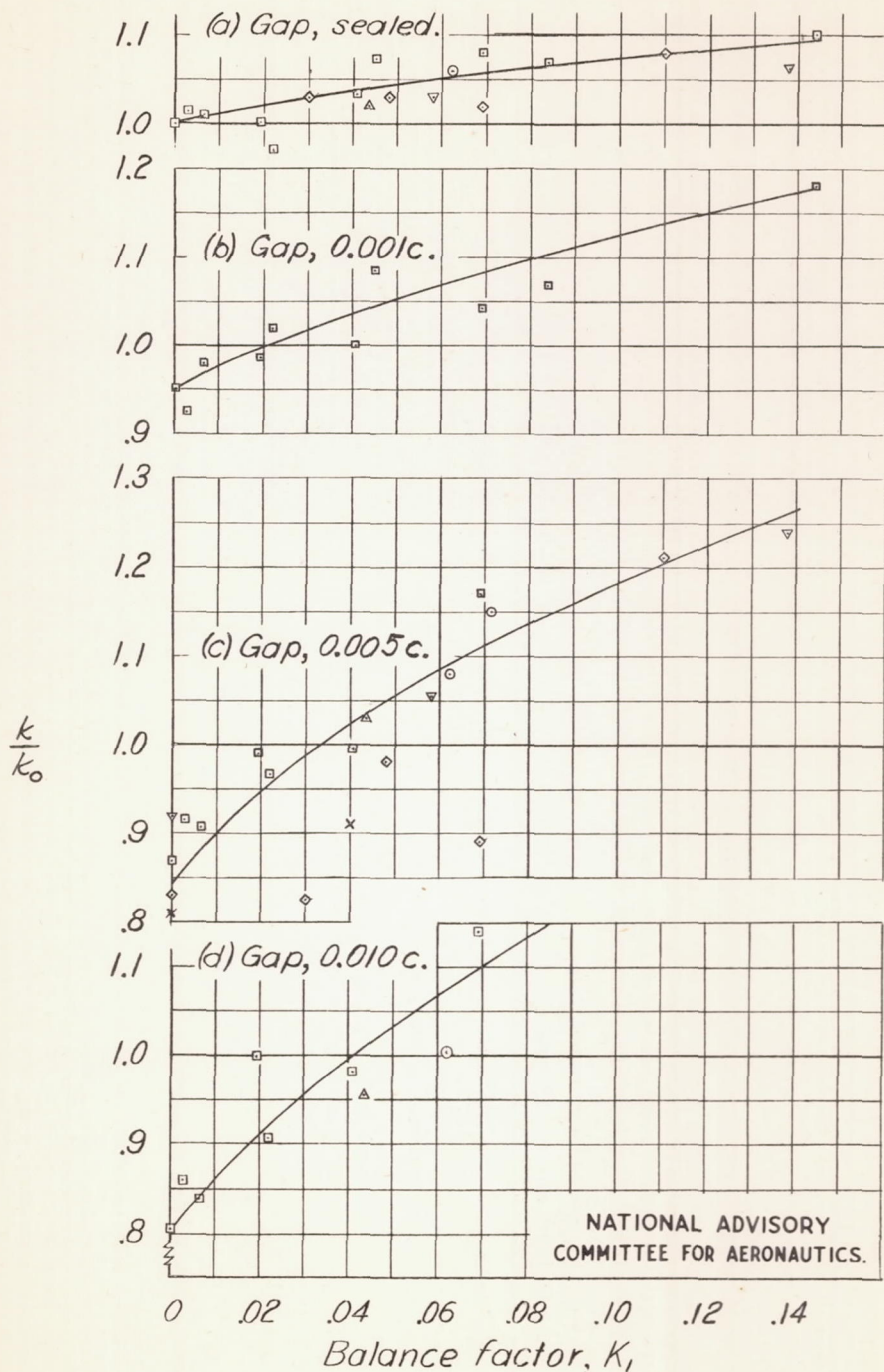
Figure 6.- Variation of lift-effectiveness parameter, relative to lift-effectiveness parameter of plain-sealed flaps, with balance factor. M, 0.1 to 0.2. Symbols are for corresponding models of table II.
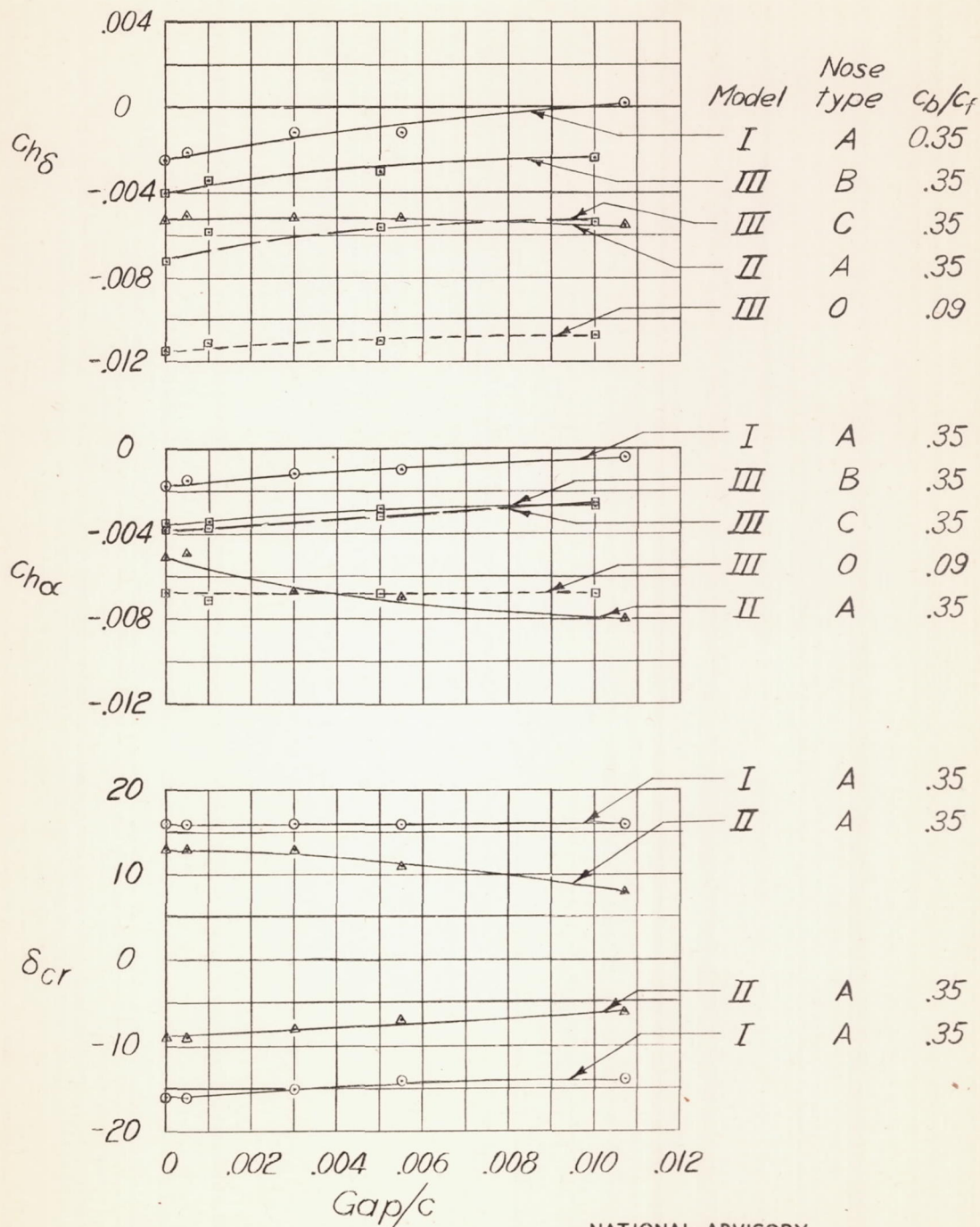
L-665

Figure 7.- Variation of flap section hinge-moment parameters
and critical deflection with gap. α, 0°; M, 0.1 to 0.2.
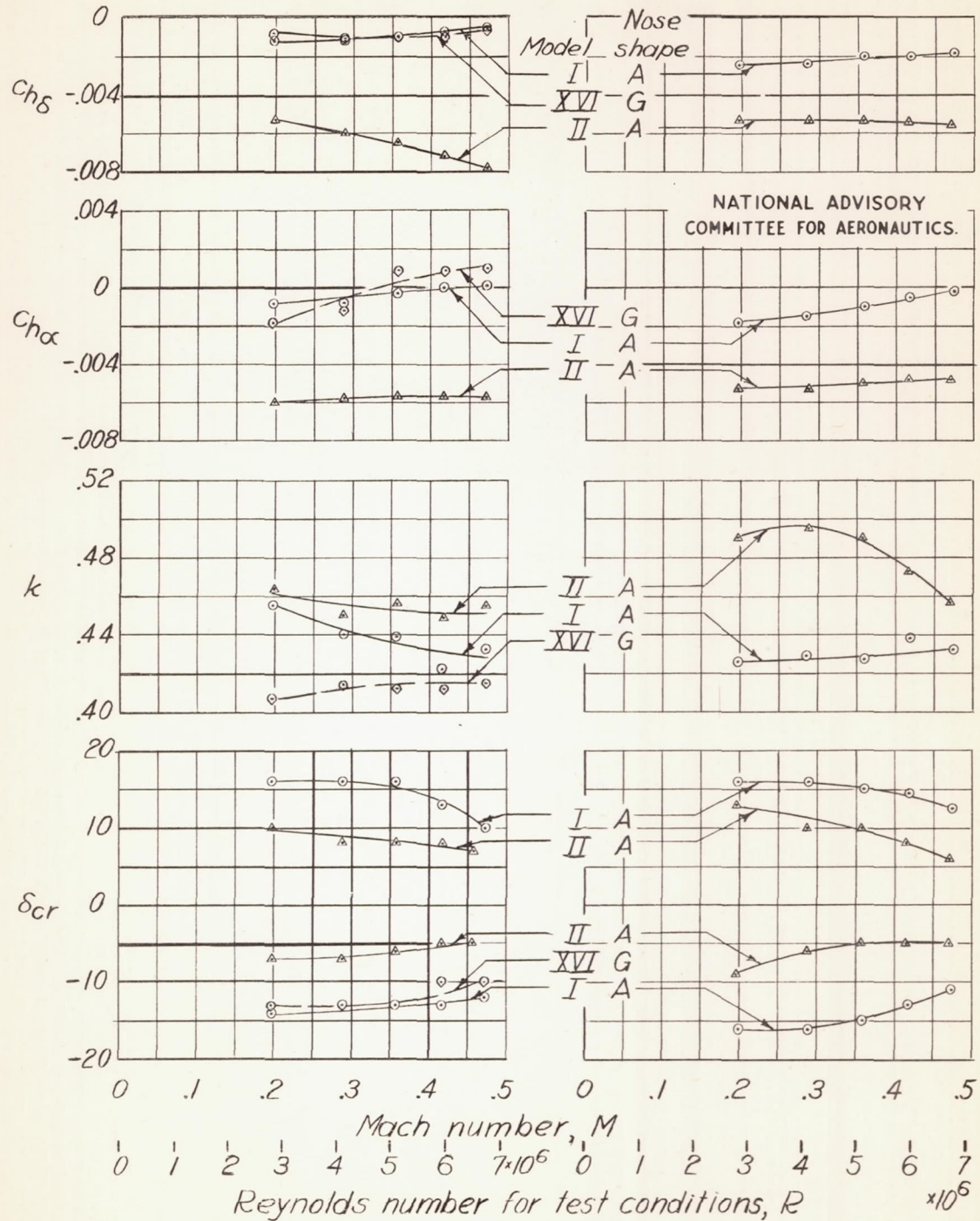
(a) Gap ≈ 0.005c.   (b) Gap, sealed.

Figure 8.— Variation of flap section hinge-moment parameters, lift-effectiveness parameter, and critical deflection with Mach number and Reynolds number. α, 0°.
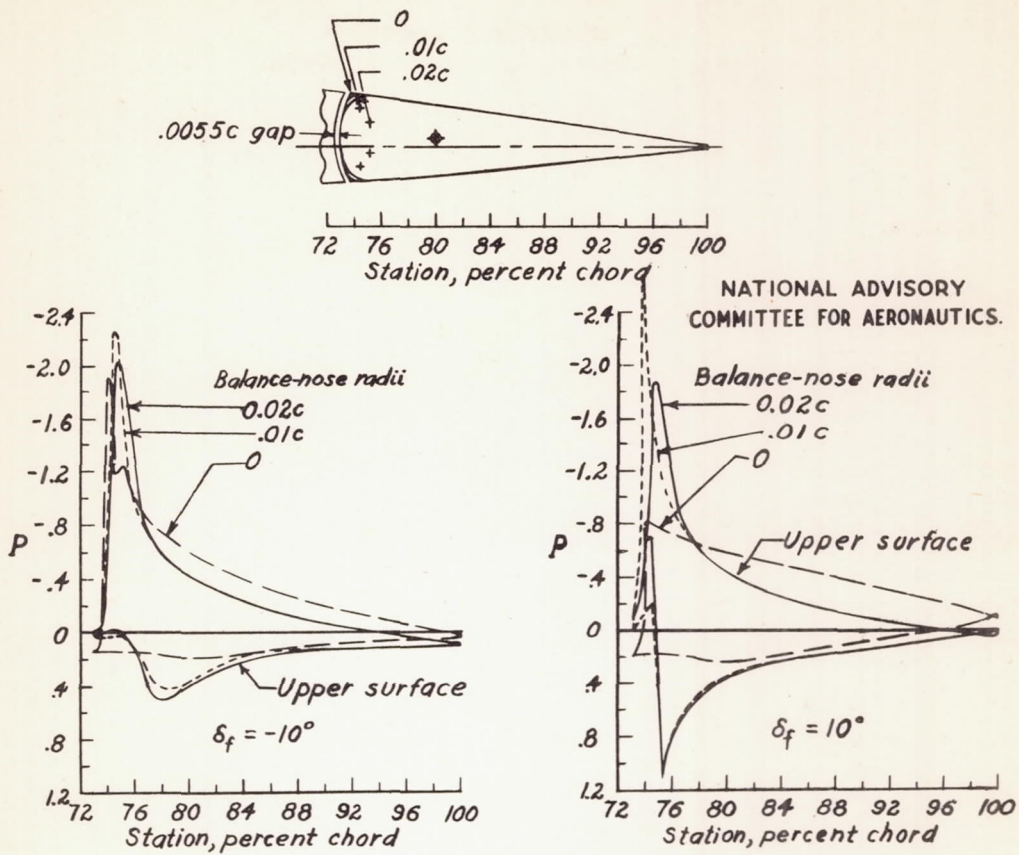
(a) Effect of balance-nose radii, 0.0055c gap open.
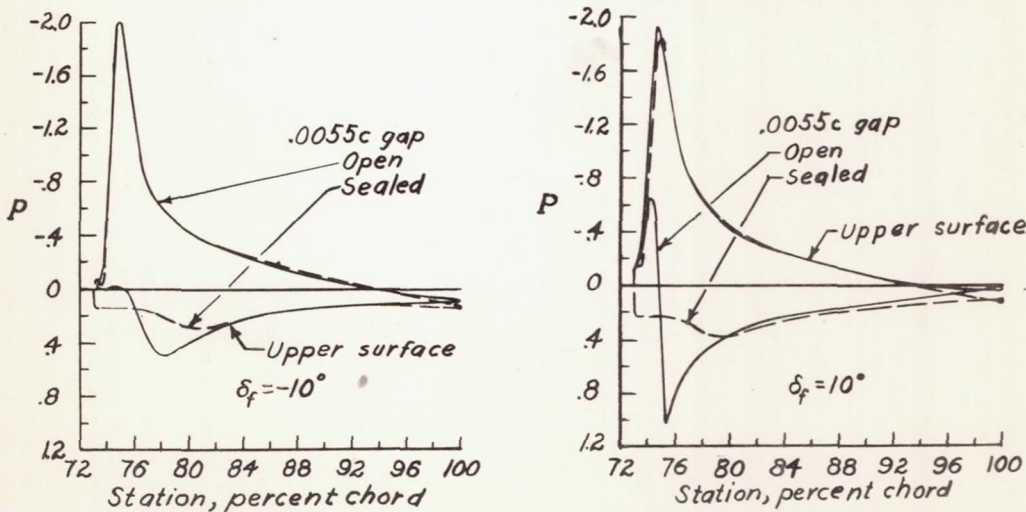
(b) Effect of seal, 0.0055c gap, 0.02c balance-nose radii.

Figure 9.- Pressure distributions on a 0.20c flap with a 0.35 c_f blunt-nose balance. NACA 23012 airfoil section (model I of table II); data from reference 26; α, 0°; M ≈ 0.36.
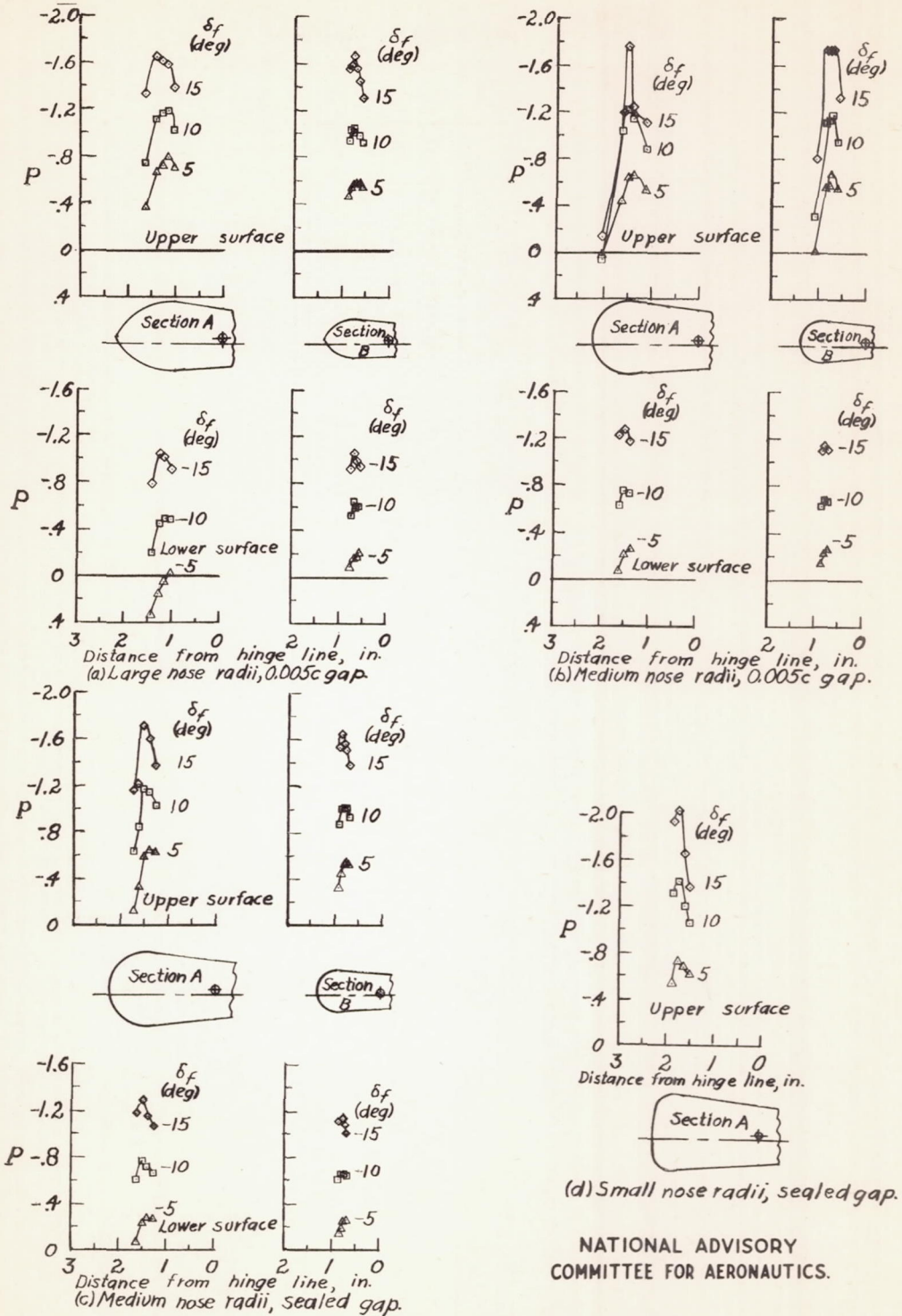
L-665

Figure 10.- Effect of aileron deflection and nose shape on the peak pressures at the nose of a 0.155c aileron with a 0.35 c_f balance. Model IX of table II; data from reference 19; α, 0°; M≈0.1 .

(a) Large nose radii, 0.005c gap.

(b) Medium nose radii, 0.005c gap.

(c) Medium nose radii, sealed gap.

(d) Small nose radii, sealed gap.
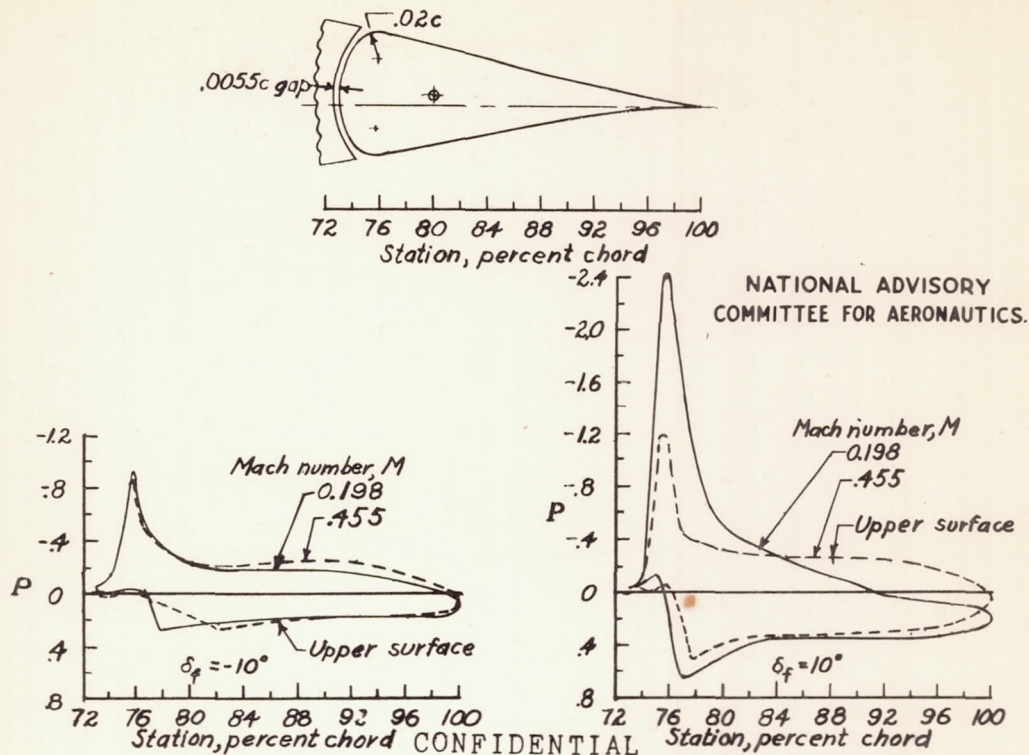
NATIONAL ADVISORY
COMMITTEE FOR AERONAUTICS.

CONFIDENTIAL

Figure 11.- Pressure distributions on a 0.20c flap with a 0.35c_f blunt-nose balance. NACA 66(215)-216, a=1.0 airfoil section; model II of table II: data from reference 26; α, 0°; gap, 0.0055c.

CONFIDENTIAL

NATIONAL ADVISORY
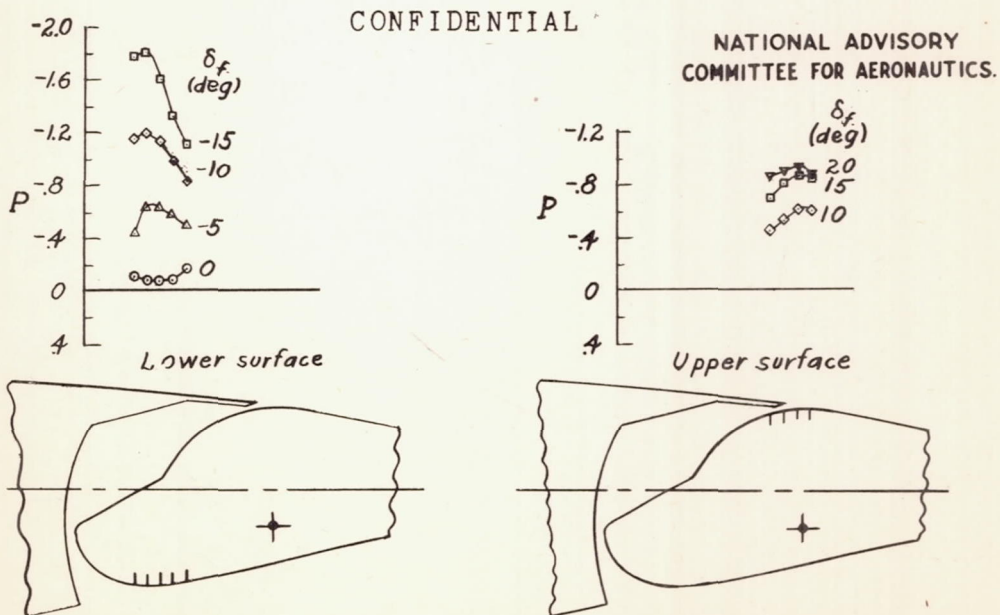COMMITTEE FOR AERONAUTICS.

Figure 12.- Effect of aileron deflection on peak pressures of a 0.20c aileron with a 0.40c_f Frise balance. Model XIX of table II. Data from reference 1; α, 1°; M ≈ 0.1.

L-665

(a) Effect of balance-nose radius, 0.0055c vent gap, 0 lower-surface radius.

NATIONAL ADVISORY
COMMITTEE FOR AERONAUTICS.

(b) Effect of vent gap and lower-surface radius, 0.008c balance-nose radius.
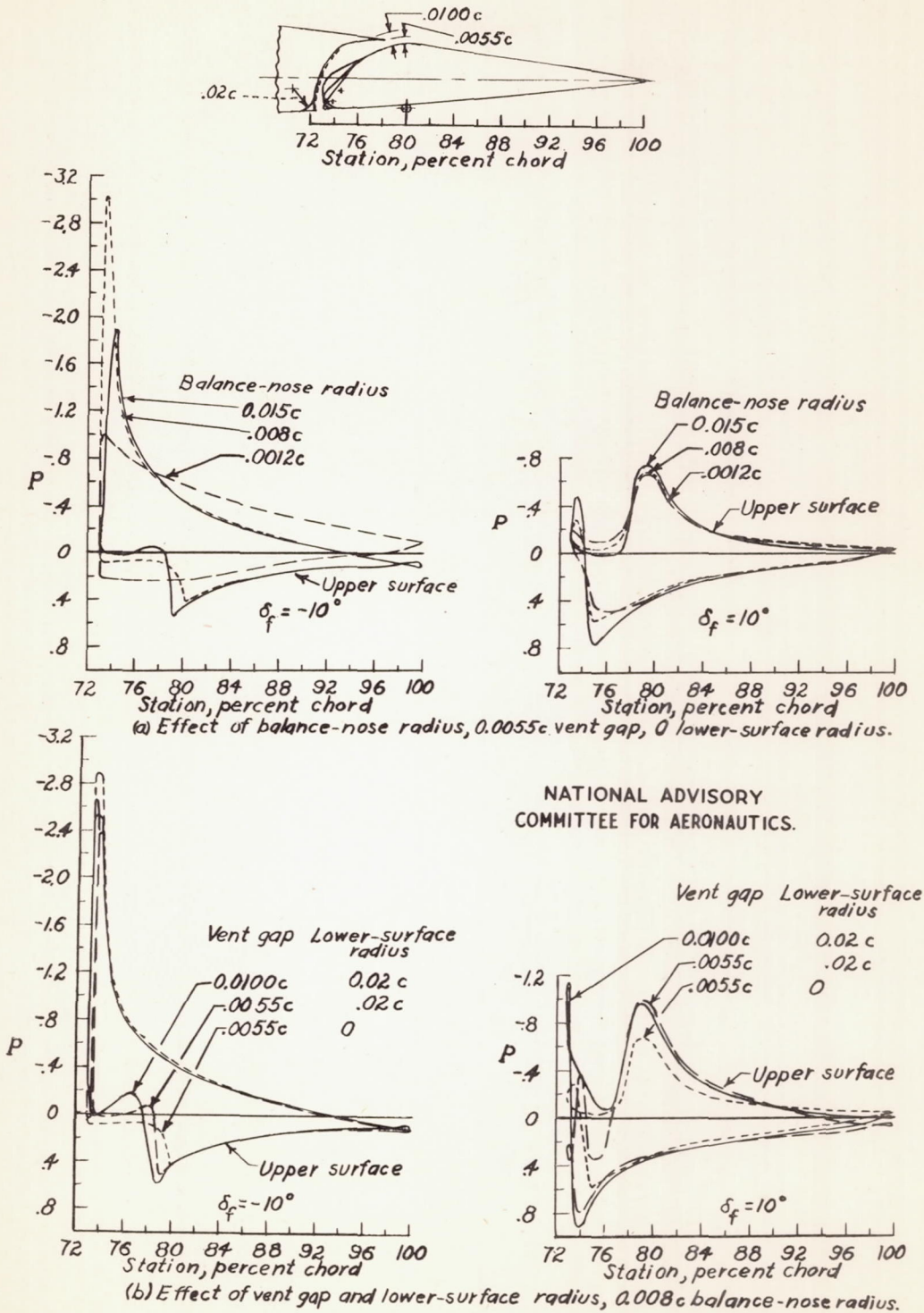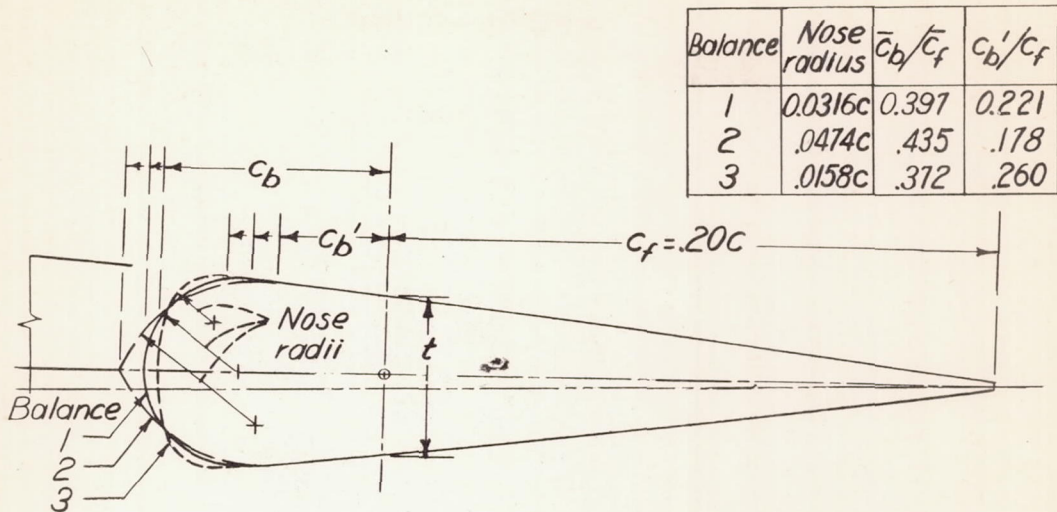
Figure 13.- Pressure distributions on a 0.20c flap with a 0.35c_f Frise balance. NACA 23012 airfoil section; model XVI of table II; data from reference 26; α, 0°; M, 0.36.

L-665

Balance	Nose radius	$\bar{c}_b/\bar{c}_f$	$\bar{c}_b'/\bar{c}_f$
1	0.0316c	0.397	0.221
2	.0474c	.435	.178
3	.0158c	.372	.260

(a) Balances having different nose radii and different overhangs but the same balance factor. K_1, 0.074; $\frac{\bar{t}/2}{\bar{c}_f}$, 0.131; estimated C_{h_δ}, -0.0011.
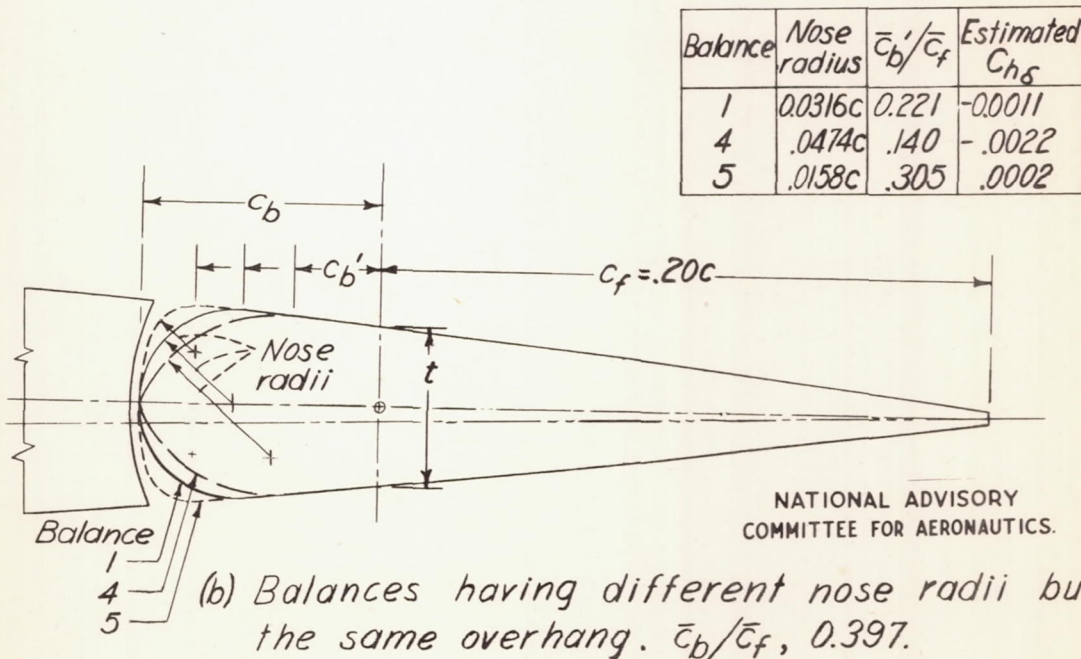
Balance	Nose radius	$\bar{c}_b'/\bar{c}_f$	Estimated C_{h_δ}
1	0.0316c	0.221	-0.0011
4	.0474c	.140	- .0022
5	.0158c	.305	.0002

NATIONAL ADVISORY
COMMITTEE FOR AERONAUTICS.

(b) Balances having different nose radii but the same overhang. $\bar{c}_b/\bar{c}_f$, 0.397.

Figure 14.- Various plain-overhang balances derived for ailerons of wing used for illustrative example. NACA 23012 airfoil ; $\bar{c}_f/\bar{c}$, 0.20 ; $\frac{\bar{t}/2}{\bar{c}_f}$, 0.131; $\bar{c}_b/\bar{c}_f$, 0.397.